NACA RM E56G31

C.1

NACA

RESEARCH MEMORANDUM

ANALYTICAL INVESTIGATION OF SINGLE-STAGE-TURBINE EFFICIENCY CHARACTERISTICS IN TERMS OF WORK AND SPEED REQUIREMENTS

By Warner L. Stewart

Lewis Flight Propulsion Laboratory
Cleveland, Ohio

CLASSIFICATION CHANGED

UNCLASSIFIED

DoA Ltr dtd effective May 16 1958
by authority of RN-127 Date OCT 22 1956
dtd 7-9-58

LIBRARY COPY

LANGLEY AERONAUTICAL LABORATORY
LIBRARY NACA
LANGLEY FIELD, VIRGINIA

CLASSIFIED DOCUMENT

This material contains information affecting the National Defense of the United States within the meaning of the espionage laws, Title 18, U.S.C., Secs. 793 and 794, the transmission or revelation of which in any manner to an unauthorized person is prohibited by law.

NATIONAL ADVISORY COMMITTEE
FOR AERONAUTICS

WASHINGTON

October 15, 1956

NASA Technical Library
3 1176 01436 1076

NACA RM E56G31

NATIONAL ADVISORY COMMITTEE FOR AERONAUTICS

RESEARCH MEMORANDUM

5048

CL-1

ANALYTICAL INVESTIGATION OF SINGLE-STAGE-TURBINE EFFICIENCY CHARACTERISTICS IN TERMS OF WORK AND SPEED REQUIREMENTS

By Warner L. Stewart

SUMMARY

This report presents an analysis of single-stage-turbine efficiency characteristics in terms of a work-speed parameter λ, defined as the ratio of the square of the mean section blade speed to the required specific work output. This parameter is the same as the familiar Parsons' characteristic number. The range of this parameter considered in the analysis included that used in turbojet engine applications as well as that used in such applications as turbopump and accessory drives. The efficiencies investigated were (a) total or aerodynamic efficiency, (b) rating efficiency (used in turbojet engine applications), and (c) static efficiency (used for turbopump and accessory drive applications). Velocity diagram types considered included zero exit whirl, impulse, as well as those corresponding to maximum values of efficiency.

The results of the analysis indicated that the total efficiency does not vary to any great extent over the range of λ used for turbojet engine applications (0.5 to 1). At reduced values of λ the total efficiency dropped off as a result of the required flow velocities being increased compared with the work output. Values of total efficiency greater than those obtained for either the zero-exit-whirl or impulse case were obtained, improvements in efficiency being of the order of 1 to 2 points. For this case, however, high values of negative exit whirl were required resulting in low rating and static efficiencies. The maximum value of rating efficiency occurred at a velocity diagram condition corresponding to a slight negative exit whirl.

In the range of λ from 0 to 0.5, where static efficiency becomes important (turbopump and accessory drive applications) the static efficiency dropped off markedly. The trends obtained compared favorably with the limited experimental data available. For a given turbine size, reduction in weight flow reduced the general level of total efficiency over the entire range of λ as a result of the increase in surface area per unit weight flow. The static efficiency, however, was approximately

independent of this variation at reduced λ values because the reduced leaving loss counterbalanced the reduction in total efficiency.

INTRODUCTION

The NACA is currently engaged in the study of the sources and significance of various losses that occur within turbine blade rows. Turbines investigated in the program thus far have been of the type suitable for turbojet engine use where relatively high blade speeds are used with comparatively moderate required specific work outputs.

Recently, considerable interest has been focused on turbines designed for such applications as turbopump and accessory drives. These turbines differ from jet engine turbines in that a high specific work output is desired at comparatively low blade speeds. The limited information available has indicated poor efficiency characteristics for this type turbine. Thus a desire for studies of the effect of the change in requirements on the turbine efficiency characteristics is indicated in order that the causes of the reduced efficiencies be understood.

This report presents an analysis of the effect of variations in the work and speed requirements on the efficiency characteristics of single-stage, full-admission turbines. The parameter λ used in computing these characteristics is the same as the familiar "Parsons' characteristic number" (ref. 1), which is defined as the ratio of the square of the design mean section blade speed to the design specific work output. The range of this parameter considered covers that encountered in jet engine applications (0.5 to 1) as well as that encountered in the accessory and pump drive turbine applications (0 to 0.5).

Three types of efficiency are considered:

(a) Total or aerodynamic efficiency which includes all aerodynamic losses (such as those due to boundary layer, tip clearance, etc.)

(b) Rating efficiency which, in addition to the aerodynamic losses, considers the whirl out of the turbine as a loss (this definition of efficiency is used in jet engine work because the energy involved in the exit whirl does not contribute to engine thrust)

(c) Static efficiency which, in addition to the aerodynamic losses, considers the total velocity head out of the turbine as a loss (this efficiency is important for accessory and pump drive turbines)

5048

5048

CL-1 back

These three efficiencies are studied for mean blade section velocity diagram types including those of zero exit whirl, impulse, and those corresponding to maximum values of efficiency.

EFFICIENCY AND VELOCITY DIAGRAM CONSIDERATIONS

As discussed in the INTRODUCTION, the parameter used herein to correlate the turbine efficiency characteristics is a function of the specific work output $\Delta h'$ and the mean section blade speed U. This parameter λ, which is the same as the Parsons' characteristic number of reference 1, can be written as

$$\lambda = \frac{U^2}{gJ\Delta h'} \tag{1}$$

All symbols are defined in appendix A.

The work-speed parameter λ defined by equation (1) is used in preference to the common blade-jet speed ratio υ, because λ is a function of the parameters usually considered turbine requirements, whereas the blade-jet speed ratio requires also a knowledge of the static efficiency, which is considered a dependant variable herein. The relation between λ and υ is described in appendix B and is used when a comparison with experimental results is made.

Efficiency Equations

The INTRODUCTION points out that three types of efficiency are considered herein. These three efficiencies, total, rating, and static, are developed in this section in terms of the work-speed parameter λ and the stator-exit whirl parameter $V_{u,1}/\Delta V_u$, which determines the type of velocity diagram used.

Total efficiency. - The total efficiency of the turbine, the efficiency that includes all the aerodynamic losses, is defined as

$$\eta_t = \frac{\Delta h'}{\Delta h'_{id}} \tag{2}$$

where $\Delta h'$ is the design specific work output and $\Delta h'_{id}$ is the ideal specific work output corresponding to the required total-pressure ratio across the turbine.

[redacted]

Equation (2) can also be written as

$$\eta_t = \frac{\Delta h'}{\Delta h' + (\Delta h'_{id} - \Delta h')} \tag{3}$$

where $\Delta h'_{id} - \Delta h'$ can be termed the loss in specific energy across the turbine. The general equation relating the specific work output, blade speed, and whirl velocities is

$$\Delta h' = \frac{U\Delta V_u}{gJ} \tag{4}$$

One can solve equation (4) for U and substitute this result into equation (1) to obtain the following equation relating λ to the specific work output and whirl velocities

$$\lambda = \frac{gJ\Delta h'}{\Delta V_u^2} \tag{5}$$

Solving equation (5) for $\Delta h'$, substituting into equation (3), and dividing by $\Delta V_u^2/gJ$ then yield

$$\eta_t = \frac{\lambda}{\lambda + \dfrac{gJ\,(\Delta h'_{id} - \Delta h')}{\Delta V_u^2}} \tag{6}$$

At this point it is assumed that the turbine specific energy loss $\Delta h'_{id} - \Delta h'$ is equal to the sum of the stator and rotor specific losses $L_S + L_R$. These blade losses, expressed in units of Btu/lb, are defined as the difference between the ideal and actual specific kinetic energy obtained through expansion to the blade-exit static pressure. The validity of this assumption is investigated in appendix C where it is shown to be correct except for the small effect of absolute enthalpy variation occurring through the turbine. With this assumption, equation (6) can be altered to

$$\eta_t = \frac{\lambda}{\lambda + \dfrac{gJ\,(L_S + L_R)}{\Delta V_u^2}} \tag{7}$$

5048

5048

It is now desired to relate the loss expression $L_S + L_R$ to the velocity diagram characteristics. In general, from boundary-layer theory it can be shown that the total loss in kinetic energy occurring in a turbine is proportional to the product of the surface area exposed to the flow and the specific kinetic energy level of the flow. That is,

$$w(L_S + L_R) \sim AE$$

or solving for $L_S + L_R$,

$$L_S + L_R \sim (A/w)E \tag{8}$$

This specific kinetic energy level E is represented herein by the average of the specific kinetic energies entering and leaving the blade rows where the velocities are relative to the blade rows. Figure 1 presents a typical set of single-stage-turbine velocity diagrams. The average stator specific kinetic energy can be written as

$$\frac{V_{x,0}^2 + V_{x,1}^2 + V_{u,1}^2}{4g}$$

and that of the rotor as

$$\frac{V_{x,1}^2 + W_{u,1}^2 + V_{x,2}^2 + W_{u,2}^2}{4g}$$

Thus

$$E = \frac{V_{x,0}^2 + 2V_{x,1}^2 + V_{u,1}^2 + W_{u,1}^2 + V_{x,2}^2 + W_{u,2}^2}{8g} \tag{9}$$

Using an average axial specific kinetic energy defined by

$$\frac{(V_x^2)_{av}}{2g} = \frac{V_{x,0}^2 + 2V_{x,1}^2 + V_{x,2}^2}{8g}$$

equation (9) can be written as

$$E = \frac{4(V_x^2)_{av} + V_{u,1}^2 + W_{u,1}^2 + W_{u,2}^2}{8g} \tag{10}$$

The following equations relate the relative tangential velocity at the rotor inlet and exit to the stator-exit whirl:

$$W_{u,1} = V_{u,1} - U$$

$$W_{u,2} = V_{u,1} - U - \Delta V_u$$

Using these relations as equation (10) is substituted into equation (8) gives .

$$L_S + L_R \sim A/w \frac{4(V_x^2)_{av} + V_{u,1}^2 + (V_{u,1} - U)^2 + (V_{u,1} - U - \Delta V_u)^2}{8g} \quad (11)$$

Finally, substituting equation (11) into equation (7) using a constant of proportionality K yields

$$\eta_t = \frac{\lambda}{\lambda + BC} \quad (12a)$$

where

$$B = K \frac{A}{w} \quad (12b)$$

$$C = 4\lambda \frac{(V_x^2)_{av}}{gJ\Delta h'} + \left(\frac{V_{u,1}}{\Delta V_u}\right)^2 + \left(\frac{V_{u,1}}{\Delta V_u} - \lambda\right)^2 + \left(\frac{V_{u,1}}{\Delta V_u} - \lambda - 1\right)^2 \quad (12c)$$

Thus for given values of K, A/w, and $(V_x^2)_{av}/gJ\Delta h'$, the total efficiency presented in equation (12a) is in terms of the desired parameters, $V_{u,1}/\Delta V_u$ and λ.

Throughout most of the analysis, K, A/w (and thus B), and $(V_x)_{av}/gJ\Delta h'$ are assumed constant. From equation (8) it can be seen that the assumption of constant A/w resolves itself into the assumption that the stator and rotor specific losses are proportional to the average specific kinetic energy level of the flow. An assumption of this type has been used extensively in predicting turbine off-design performance characteristics (refs. 2 and 3). The success of these predictions suggests that this assumption should also be valid when studying design-point efficiency characteristics. The effect of increasing A/w through reduction in the axial component of velocity as well as the general effect of varying K is discussed toward the end of the report.

5048

5048

Rating efficiency. - As indicated in the INTRODUCTION, when a turbine is used in a jet engine, the kinetic energy involved in the turbine-exit whirl is considered a loss, because this energy does not contribute to engine thrust. Thus, a so-called rating efficiency that considers this additional loss is in considerable use in the field. The equation for the rating efficiency η_x is

$$\eta_x = \frac{\Delta h'}{\Delta h'_{id,x}} \tag{13}$$

Figure 2 presents the familiar enthalpy-entropy diagram with the turbine characteristics shown. From this figure,

$$\Delta h'_{id,x} = \Delta h'_{id} + L_u \tag{14}$$

The energy represented by the length L_u and the kinetic energy of the turbine-exit tangential velocity $V_{u,2}^2/2gJ$ can both be considered as isentropic changes in enthalpy between pressures p'_2 and $p'_{x,2}$. The ratios of these isentropic enthalpy changes to their initial enthalpy levels are, therefore, the same. That is,

$$\frac{L_u}{h'_{id,2}} = \frac{\frac{V_{u,2}^2}{2gJ}}{h'_2} \tag{15}$$

solving equation (15) for L_u and substituting the result into equation (14) give

$$\Delta h'_{id,x} = \Delta h'_{id} + \frac{h'_{id,2}}{h'_2}\left(\frac{V_{u,2}^2}{2gJ}\right) \tag{16}$$

Then substituting equation (16) into equation (13) yields

$$\eta_x = \frac{\Delta h'}{\Delta h'_{id} + \frac{h'_{id,2}}{h'_2}\left(\frac{V_{u,2}^2}{2gJ}\right)} \tag{17}$$

It is assumed that

$$\frac{h'_{id,2}}{h'_2} \approx 1 \tag{18}$$

since no actual enthalpy levels are used. The error in η_x as a result of this assumption was studied, and it was found that this error would result in a maximum difference of less than 3 percentage points in efficiency in the practical range of λ ($\lambda > 0.1$).

In comparing the rating efficiency η_x with the total efficiency η_t, let equation (17) as modified by equation (18) be divided by $\Delta h'_{id}$ to yield

$$\eta_x = \frac{\eta_t}{1 + \frac{V_{u,2}^2}{2gJ\Delta h'_{id}}} \tag{19}$$

Finally, by using the equation

$$V_{u,2} = V_{u,1} - \Delta V_u \tag{20}$$

together with equations (2) and (5), equation (19) can be altered to

$$\eta_x = \frac{\eta_t}{1 + \frac{\eta_t}{2\lambda}\left(\frac{V_{u,1}}{\Delta V_u} - 1\right)^2} \tag{21}$$

Thus once η_t is known for given values of λ and $V_{u,1}/\Delta V_u$, η_x can be computed.

Static efficiency. - In many applications such as turbopump and auxiliary drives, the entire kinetic energy leaving the turbine is considered lost and the performance is based on the total- to static-pressure ratio across the turbine. From these considerations an equation similar to equation (17) can be derived as

$$\eta_s = \frac{\Delta h'}{\Delta h'_{id} + \frac{h'_{id,2}}{h'_2}\left(\frac{V_2^2}{2gJ}\right)} \tag{22}$$

Using the same assumption made for the rating efficiency, equation (22) can be modified to

$$\eta_s = \frac{\eta_t}{1 + \frac{\eta_t}{2}\left[\frac{1}{\lambda}\left(\frac{V_{u,1}}{\Delta V_u} - 1\right)^2 + \frac{V_{x,2}^2}{gJ\Delta h'}\right]} \tag{23}$$

[redacted]

5048

5048

CL-2

In presenting static efficiency characteristics, $V_{x,2}^2$ is assumed equal to $(V_x^2)_{av}$. In general, the axial component of velocity increases from the turbine inlet to exit so that using $(V_x^2)_{av}$ yields static efficiencies somewhat higher than that computed using $V_{x,2}^2$.

Velocity Diagram Considerations

For a given value of λ a variety of velocity diagrams can be devised that satisfy the turbine requirements. Variations in the velocity diagram characteristics can be made by varying the stator-exit whirl parameter $V_{u,1}/\Delta V_u$. For the velocity diagram calculation presented in this section, the parameter $(V_x^2)_{av}/gJ\Delta h'$ was selected as 0.49, because this value corresponds approximately with that being encountered in a number of turbojet engine turbines being investigated at the Lewis laboratory. A value for B of 0.030 was then selected, since this value yielded total efficiency levels comparable with those obtained experimentally for these turbines. Although the results of the calculations based on these values are presented in this section, comparison of these results is reserved for the EFFICIENCY COMPARISONS section.

Zero exit whirl. - In many cases it is desired to specify zero exit whirl or $V_{u,2} = 0$ because in this case

$$\eta_t = \eta_x$$

As a result,

$$\frac{V_{u,1}}{\Delta V_u} = 1 \tag{24}$$

Substituting equation (24) into equations (12a) and (23) and simplifying yield

$$\eta_t = \eta_x = \frac{\lambda}{\lambda + 2B\left[2\lambda \frac{(V_x^2)_{av}}{gJ\Delta h'} + 1 - \lambda + \lambda^2\right]} \tag{25}$$

and

$$\eta_s = \frac{\eta_t}{1 + \frac{\eta_t}{2} \frac{(V_x^2)_{av}}{gJ\Delta h'}} \tag{26}$$

The efficiency characteristics for the zero-exit-whirl case as computed from equations (25) and (26) are presented in figure 3 where efficiency is presented as a function of λ. As is shown later, impulse conditions across the rotor occur for this case at $\lambda = 0.5$ with positive reaction at $\lambda > 0.5$ and negative reaction at $\lambda < 0.5$. This negative-reaction area is shaded in figure 3 to represent an undesirable area of operation because experience has indicated abnormally increased blade losses when negative reaction is encountered.

5048

Impulse conditions. - The specification of impulse conditions across the rotor defines equal relative velocities at the rotor entrance and exit. Thus if the axial component of velocity at the rotor entrance and exit are assumed equal,

$$W_{u,1} = - W_{u,2}$$

Since

$$\Delta V_u = W_{u,1} - W_{u,2}$$

the equation

$$W_{u,1} = \frac{\Delta V_u}{2}$$

can be obtained. Finally, since

$$V_{u,1} = U + W_{u,1}$$

the equation

$$\frac{V_{u,1}}{\Delta V_u} = \lambda + \frac{1}{2} \tag{27}$$

can be obtained. Equation (27) relates the stator-exit whirl parameter to the work-speed parameter for impulse conditions. Substituting this equation into equations (12a), (21), and (23) yields

$$\eta_t = \frac{\lambda}{\lambda + B\left[4\lambda \frac{(V_x^2)_{av}}{gJ\Delta h'} + \lambda^2 + \lambda + \frac{3}{4}\right]} \tag{28}$$

5048 CL-2 back

$$\eta_x = \frac{\eta_t}{1 + \frac{\eta_t}{2\lambda}\left(\lambda - \frac{1}{2}\right)^2} \tag{29}$$

$$\eta_s = \frac{\eta_t}{1 + \frac{\eta_t}{2}\left[\frac{1}{\lambda}\left(\lambda - \frac{1}{2}\right)^2 + \frac{(V_x^2)_{av}}{gJ\Delta h'}\right]} \tag{30}$$

Equations (28), (29), and (30) are graphically illustrated in figure 4. It can be seen that $\eta_x = \eta_t$ only at $\lambda = 0.5$ which would represent the zero-exit-whirl case. The rating efficiency is reduced considerably from the total efficiency as λ increases or decreases from 0.5. This occurs because large positive exit whirls at $\lambda > 0.5$ and large negative exit whirls at $\lambda < 0.5$ are required to maintain the impulse condition. These whirl characteristics can be seen more clearly in figure 5 where the turbine-exit whirl parameter $V_{u,2}/\Delta V_u$ is presented as function of λ for a number of different velocity diagram types. The impulse case (running from -0.5 at $\lambda = 0$ to +0.5 at $\lambda = 1$) represents the demarkation line between positive and negative reaction. The area to the left and above the impulse curve is hatched to represent the undesired negative reaction range. The other parts of this figure are discussed in the next two sections.

In the discussion of the impulse conditions it should be noted that only mean section conditions are considered. In an actual turbine, radial variations in V_u occur in order to satisfy radial equilibrium. Thus an impulse condition at the mean radius would result in negative reaction at the hub. This indicates that a condition of positive reaction at the mean radius should be selected if a reaction limit of impulse is specified for the whole rotor. Another factor to consider, however, is that, for the mean radius impulse condition considered herein, a constant axial velocity was assumed, whereas in most turbines the axial velocity increases across the rotor. Thus an impulse condition considered herein would correspond to some positive reaction in an actual turbine. Because the effects just discussed counterbalance each other, the λ value at which impulse occurs herein should closely approximate the λ value at which impulse occurs at the root of an actual rotor.

Maximum total efficiency. - The specification of the zero-exit-whirl or impulse condition determines specific values of $V_{u,1}/\Delta V_u$ for a given λ. If the complete range of $V_{u,1}/\Delta V_u$ (0 to 1) is covered for a given λ, a variation in total efficiency similar to that of figure 6 would be obtained, in this case for $\lambda = 0.25$ (the rating efficiency curve is

discussed later). It can be seen from this figure that there is a maximum total efficiency at a stator-exit whirl parameter less than that for either the zero-exit-whirl or impulse case. Investigation of this maximum total efficiency can be made using equation (12a). For specified values of λ and B, the maximum total efficiency would occur when C is a minimum. So, the partial derivative of C can be taken with respect to $V_{u,1}/\Delta V_u$ to yield

$$\frac{\partial C}{\partial\left(\frac{V_{u,1}}{\Delta V_u}\right)} = 2\,\frac{V_{u,1}}{\Delta V_u} + 2\left(\frac{V_{u,1}}{\Delta V_u} - \lambda\right) + 2\left(\frac{V_{u,1}}{\Delta V_u} - \lambda - 1\right)$$

Setting this equation equal to zero and solving for $V_{u,1}/\Delta V_u$ gives

$$\left(\frac{V_{u,1}}{\Delta V_u}\right)_{\max \eta_t} = \frac{2\lambda + 1}{3} \tag{31}$$

With equation (31), the total, rating, and static efficiencies were computed using equations (12a), (21), and (23) with the results presented in figure 7. At reduced values of λ, the rating and static efficiencies decrease rapidly. The reason for this trend can be seen from figure 5 where it is indicated that the maximum total efficiency occurs at very high negative exit whirls for low values of λ. It might also be noted that $\eta_{t,max}$ corresponds to the zero-exit-whirl case at $\lambda = 1$.

Maximum rating efficiency. - Figure 6 also presents a typical variation in rating efficiency η_x with $V_{u,1}/\Delta V_u$ for a given λ. It can be seen that η_x also reaches a maximum at some value of $V_{u,1}/\Delta V_u$ different from those for the cases of zero exit whirl, impulse, and maximum total efficiency. To explore this maximum-rating-efficiency case equation (21) can be rewritten

$$\eta_x = \frac{1}{\frac{1}{\eta_t} + \frac{1}{2\lambda}\left(\frac{V_{u,1}}{\Delta V_u} - 1\right)^2} \tag{32}$$

Substituting equation (12a) into equation (32) then yields

$$\eta_x = \frac{1}{1 + \frac{BC}{\lambda} + \frac{1}{2\lambda}\left(\frac{V_{u,1}}{\Delta V_u} - 1\right)^2}$$

or

5048

$$\eta_x = \frac{1}{1 + \frac{B}{\lambda}\left[4\lambda \frac{(V_x^2)_{av}}{gJ\Delta h'} + \left(\frac{V_{u,1}}{\Delta V_u}\right)^2 + \left(\frac{V_{u,1}}{\Delta V_u} - \lambda\right)^2 + \left(\frac{V_{u,1}}{\Delta V_u} - \lambda - 1\right)^2 + \frac{1}{2B}\left(\frac{V_{u,1}}{\Delta V_u} - 1\right)^2\right]}$$

5048

Now η_x is a maximum when the expression within the brackets is a minimum. So taking the partial derivative of this expression with respect to $V_{u,1}/\Delta V_u$

$$\frac{\partial[\ ]}{\partial\left(\frac{V_{u,1}}{\Delta V_u}\right)} = 2\left(\frac{V_{u,1}}{\Delta V_u}\right) + 2\left(\frac{V_{u,1}}{\Delta V_u} - \lambda\right) + 2\left(\frac{V_{u,1}}{\Delta V_u} - \lambda - 1\right) + \frac{2}{2B}\left(\frac{V_{u,1}}{\Delta V_u} - 1\right)$$

Setting this equation equal to zero and solving for $V_{u,1}/\Delta V_u$ give

$$\left(\frac{V_{u,1}}{\Delta V_u}\right)_{\max \eta_x} = \frac{2\lambda + 1 + \frac{1}{2B}}{3 + \frac{1}{2B}} \tag{33}$$

The efficiency characteristics as computed using equation (33) are presented in figure 8. It is interesting to note from this figure that the value of λ where impulse conditions are reached is less for the maximum η_x case than for the zero-exit-whirl case. This can also be seen in figure 5 where the exit whirl characteristics are compared. There it can be seen that the maximum rating efficiency occurs at a small negative exit whirl with the magnitude of this whirl depending on the particular value of λ. The impulse limit of $\lambda = 0.44$ indicated in both figure 5 and figure 8 could be computed by setting equation (27) equal to equation (33) and solving for λ.

Maximum static efficiency. - In determining the velocity diagram conditions under which maximum static efficiency is obtained, an approach can be made similar to that used to obtain the conditions for maximum rating efficiency. When this was done it was found that the equation relating the stator-exit whirl parameter and λ was the same as that obtained for maximum rating efficiency (eq. (33)). The reason for the diagram characteristics being identical can be seen by comparing efficiency equations (21) and (23). The only difference in these two equations is that $V_{x,2}^2/gJ\Delta h'$ appears in the denominator of equation (23). Since this term is considered constant in this section, similar velocity diagrams for maximum values of η_x and η_s would be expected.

EFFICIENCY COMPARISONS

In this section comparison is made of the efficiency characteristics, as obtained for the various velocity diagram cases just considered. The portions of the curves representing negative reaction are excluded. As indicated previously, for all these calculations $B = 0.030$ and $\frac{(V_x^2)_{av}}{gJ\Delta h'} = 0.49$.

5048

Total Efficiency

Figure 9 presents a comparison of the total efficiency characteristics for the four velocity diagram types studied. The impulse curve of course limits the zero-exit-whirl and maximum η_x curves to values above 0.5 and 0.44, respectively.

Inspection of figure 9 reveals very little variation in total efficiency level over a wide range of λ. For example, the total efficiency varies only three percentage points between λ values of 0.5 and 1.0. As λ is reduced from 0.5 the total efficiency drops off markedly. This occurs because at reduced λ values the blade speed is low compared to the required specific work output (eq. (1)). As a result the whirl velocities must increase in comparison with the required specific work output (eq. (4)). These increased whirl velocities in turn increase the average specific kinetic energy level and hence increase the blade losses (eq. (8)). The efficiency is thus reduced because of the losses increasing compared with the required specific work output.

Figure 9 also indicates that, except for the impulse case, there is little difference among all the curves at λ values above 0.5. In fact, as λ approaches 1, these curves approach the same value. Because of the impulse case lying below the other curves when considering η_t together with comparisons to be made on other efficiency bases, the impulse case is rarely considered for $\lambda \rightarrow 0.5$.

At the low values of λ only the impulse and maximum-total-efficiency cases are presented because negative reaction is encountered for the other cases. The impulse case is 1 to 2 points lower in efficiency than the maximum-total-efficiency case.

Rating Efficiency

Figure 10 presents a comparison of the rating efficiency characteristics obtained for the four velocity diagram cases. It can be seen that, in the range of λ from 0.5 to 1 where this type efficiency is

5048

important (turbojet engine application), the rating efficiency curves for the zero-exit-whirl and maximum-rating-efficiency cases are quite flat, varying from 0.87 at $\lambda = 0.5$ to approximately 0.89 at $\lambda = 1$. The zero-exit-whirl curve is only slightly lower than that for maximum η_x, being of the order of 1/2 percentage point at $\lambda = 0.5$. Because of the high positive whirls required for the impulse and high negative whirls for the maximum η_t case, the corresponding rating efficiencies are below those of the other two cases in this range of λ (0.5 to 1). At values of λ below 0.44 the impulse case yields the maximum rating efficiency with the maximum η_t case lying far below the impulse case as a result of the higher required values of negative exit whirl.

Although efficiencies greater than those corresponding to impulse conditions would obviously have been obtained using the maximum rating efficiency case, such data are not shown because of the reaction limit imposed.

Static Efficiency

A comparison of the static efficiency characteristics can be made using figure 11. The trends are identical with those observed for the rating efficiency case; however, the level of efficiency is considerably lower because of the kinetic energy involved in the exit axial velocity. It might also be noted that in the range of λ from 0 to 0.5, where this efficiency becomes important (turbopump and accessory drives), the static efficiency drops off very rapidly. Considering the impulse case, for example, the static efficiency is less than 0.50 at λ values below 0.14.

EFFECT OF VARIATIONS IN $(V_x^2)_{av}/gJ\Delta h'$, A/w, AND K ON EFFICIENCY CHARACTERISTICS

The analysis results presented up to this point were obtained for constant values of $B = K\frac{A}{w}$ and $(V_x^2)_{av}/gJ\Delta h'$. The effect of changes in these parameters on the efficiency characteristics are considered in the next two sections. The combined effect of varying A/w and $(V_x^2)_{av}/gJ\Delta h'$ is described first. Then the general effect of varying K is discussed.

Effect of Varying A/w and $(V_x^2)_{av}/gJ\Delta h'$ on Efficiency Characteristics

One of the characteristics of accessory drive turbines is that the weight flow is small compared with that obtained in turbojet applications. The effect of the reduction in weight flow on the parameters A/w and $(V_x^2)_{av}/gJ\Delta h'$ can be considered using figure 12 where two stator blade rows are presented. These blade rows are of similar profiles but set at different stagger angles as a result of stator B being designed to pass less weight flow. As indicated by the velocity diagrams in figure 12, these stators are both required to develop the same exit whirl. Since the surface area is constant,

$$\frac{A}{w} \sim \frac{1}{w}$$

From the velocity diagrams in figure 12 it can be seen that the reduction in weight flow is manifested in terms of the reduction in V_x (neglecting the effect of density variation). That is,

$$V_x \sim w$$

From these considerations and representing V_x by $\sqrt{(V_x^2)_{av}}$ it follows that

$$\frac{A}{w} \sim \frac{1}{\sqrt{(V_x^2)_{av}}}$$

Thus, if K is held constant,

$$B = K\frac{A}{w} \sim \frac{1}{\sqrt{(V_x^2)_{av}}} \tag{34}$$

The effect of the variation in A/w and $(V_x^2)_{av}$ as prescribed by equation (34) is presented in figure 13. The zero-exit-whirl case is presented for $\lambda > 0.5$ and the impulse case shown for $\lambda < 0.5$. From this figure, it can be seen that, when considering the total efficiency characteristics, the general effect of reducing the weight flow (by increasing A/w and reducing $(V_x^2)_{av}$) is to lower the efficiency. This trend occurs because the reduction in the parameter C (eq. (12b)) through the reduction in $(V_x^2)_{av}$, which tends to improve the efficiency, is more than compensated for by the increase in B due to increasing A/w.

5048

Further inspection of figure 13 reveals that, when considering the static efficiency characteristics, the trend depends on the range of λ considered. For λ values greater than 0.4, reductions in weight flow result in a net improvement in static efficiency because the drop in total efficiency is more than compensated for by the reduction in exit kinetic energy. At λ values below 0.4 the loss in total efficiency is approximately cancelled by the increase in efficiency resulting from the reduction in exit kinetic energy and, therefore, the static efficiency is approximately independant of axial velocity level for λ values less than 0.4.

5048

CL-3

Effect of Variation in K

All of the analytical results presented in this report are for a given K. If this constant of proportionality were varied the effect would be to change the level of efficiency without altering the trends. This occurs, of course, because K appears in only one place in equation (12a) and is, therefore, uncompensated.

Variations in K would occur as a result a number of factors including the following:

(a) Compromising a design for mechanical reasons which would increase losses and, hence, the magnitude of K

(b) Designs that have considerable variation in inner- and outer-wall contouring which could result in additional losses and hence increase K

(c) Effects of Reynolds number, a reduction of which would increase K

(d) Use of parital admission which would introduce eddy losses and require an increase in K

The value of K was assumed constant implicitly by assuming $B = 0.030$ as a base value and then varying B with A/w when the effect of varying A/w was studied. As is pointed out in the next section, the level of B, and hence K, was selected using the efficiency levels obtained from single-stage full-admission turbines of clean aerodynamic design. Thus, this constant of proportionality K, used implicitly herein, would be close to the minimum encountered. It would then be expected that many experimental points would fall below the theoretical curves as a result of increased K values occurring for reasons such as those just outlined.

COMPARISON WITH EXPERIMENTAL RESULTS

A comparison between the theoretical total efficiencies obtained herein and those obtained experimentally in other investigations is shown in figure 14. These experimental results were obtained from single-stage cold-air turbines suitable for jet engine applications. The turbines were 14 to 16 inches in diameter with cylindrical inner and outer walls and clean aerodynamic design. The two theoretical curves presented are for zero exit whirl at $\lambda > 0.5$ and impulse at $\lambda < 0.5$. In comparing the experimental points with the theoretical curve it must be remembered that the value of B (0.030) was chosen to yield levels of efficiency comparable with those obtained experimentally. From figure 14, however, it can be seen that the trends of the curves are duplicated very closely by the experimental points. Although some scatter would be expected as more experimental points are added, the loss assumptions made in the analysis appear to be satisfactory, at least for the range of λ above 0.45.

5048

Very little experimental data is available for a comparison with the theoretical results at reduced values of λ. The available comparisons are made in terms of static efficiency because this efficiency is of most interest for low values of λ. The experimental results of the two single-stage turbines presented in reference 4 as well as those of a single-stage partial-admission turbine, to be compared herein, are in terms of blade-jet speed ratio. In order to correlate this data with the work-speed parameter λ, equation (B5) of appendix B was used in figure 15 to present graphically the relation between the work-speed parameter λ and the blade-jet speed ratio v. Superimposed on the graph is a theoretical curve of representative values of static efficiency for $\lambda < 0.4$ as obtained from figure 13. The circles on the figure represent the design-point performance characteristics of the two 4-inch turbines investigated in reference 4. Since no design point was specified for the partial-admission turbine, the squares present the blade efficiency characteristics over a range of blade-jet speed ratio for a total- to static-pressure ratio of 8. In general, it can be seen that, although the level of static efficiency obtained experimentally is somewhat below the theoretical curve, the trend with λ is similar to that obtained theoretically. One reason for the difference in level is that the turbine-exit axial velocity obtained experimentally was probably greater than the average occurring across the turbine, which would then yield lower static efficiencies than predicted. Other reasons would include Reynolds number effect for the small turbines of reference 4 and partial-admission effects for the other turbine (see previous section).

5048

CL-3 back

SUMMARY OF RESULTS

An analytical investigation of the effect of work and speed requirements on single-stage full-admission turbine efficiency characteristics has been presented. The range of work-speed parameter λ covered that used for turbojet engine applications as well as that for accessory and turbopump drive applications. The following summarizes the pertinent results:

1. The total efficiency did not vary to any great extent in the range of λ used for turbojet engine applications (0.5 to 1) where flow conditions close to zero exit whirl are desired. The trends obtained theoretically were verified experimentally. As λ decreased below 0.5 the total efficiency reduced considerably as a result of the required flow velocities being increased compared with the work output. A maximum value of total efficiency occurred with improvements in efficiency of the order of 1 to 2 percentage points over that obtained in the impulse or zero-exit-whirl case. Unfortunately, this maximum total efficiency occurred at velocity diagram conditions corresponding to high values of negative exit whirl.

2. A maximum value of rating efficiency occurred at a velocity diagram condition corresponding to a small amount of negative exit whirl. Maximum rating efficiency values were not considered at λ values below 0.44 as a result of the reaction limitation imposed.

3. The static efficiency decreased rapidly below a λ of 0.5 where this type efficiency becomes important (turbopump and accessory drive applications). The theoretical trends compared favorably with the limited experimental data available.

4. For a given turbine size a reduction in weight flow reduced the general level of total efficiency over the entire range of λ as a result of the increase in surface area per unit weight flow. The static efficiency, however, remained approximately constant at reduced λ values, because the reduced leaving loss approximately counterbalanced the reduction in total efficiency.

Lewis Flight Propulsion Laboratory
National Advisory Committee for Aeronautics
Cleveland, Ohio, July 25, 1956

[redacted]

APPENDIX A

SYMBOLS

5048

The following symbols are used in this report:

A turbine blade surface area, sq ft

B parameter equal to $K\frac{A}{w}$

C parameter equal to

$$4\lambda \frac{(V_x^2)_{av}}{gJ\Delta h'} + \left(\frac{V_{u,1}}{\Delta V_u}\right)^2 + \left(\frac{V_{u,1}}{\Delta V_u} - \lambda\right)^2 + \left(\frac{V_{u,1}}{\Delta V_u} - \lambda - 1\right)^2$$

E specific kinetic energy level

g acceleration due to gravity, 32.17 ft/sec^2

h specific enthalpy, Btu/lb

J mechanical equivalent of heat, 778.2 ft-lb/Btu

K constant of proportionality

L loss in kinetic energy, Btu/lb

p pressure, lb/sq ft

T temperature, $^{\circ}R$

U mean section blade speed, ft/sec

V absolute gas velocity, ft/sec

V_j ideal gas velocity corresponding to total- to static-pressure ratio across turbine, ft/sec

W relative gas velocity, ft/sec

w weight-flow rate, lb/sec

γ ratio of specific heats

η_s static efficiency, based on total- to static-pressure ratio across turbine

[redacted]

η_t total efficiency, based on total-pressure ratio across turbine

η_x rating efficiency, based on total pressure upstream of turbine and pressure downstream of turbine equal to sum of static pressure and axial component of velocity head

5048

λ work-speed parameter, $U^2/gJ\Delta h'$

υ blade-jet speed ratio, U/V_j

Subscripts:

av average

id ideal

R rotor

S stator

s static

u tangential component

x axial component

0 upstream from turbine

1 station between stator and rotor

2 downstream from turbine

Superscripts:

' absolute total state

" relative total state

5048

APPENDIX B

RELATION BETWEEN WORK-SPEED PARAMETER AND BLADE-JET SPEED RATIO

The work-speed parameter λ used in this report is defined as

$$\lambda = \frac{U^2}{gJ\Delta h'} \tag{1}$$

In order to relate this parameter to the common blade-jet speed ratio υ, let the ideal specific work output $\Delta h'_{id,s}$, corresponding to the total-to static-pressure ratio across the turbine, be introduced in equation (1), resulting in

$$\lambda = \frac{U^2}{gJ\Delta h'_{id,s}\left(\frac{\Delta h'}{\Delta h'_{id,s}}\right)} \tag{B1}$$

This ideal specific work output $\Delta h'_{id,s}$ can be expressed in terms of kinetic energy using a theoretical jet velocity V_j as

$$gJ\Delta h'_{id,s} = V_j^2/2 \tag{B2}$$

Also by definition,

$$\eta_s = \frac{\Delta h'}{\Delta h'_{id,s}} \tag{B3}$$

Therefore, substituting equations (B2) and (B3) into equation (B1) and rearranging terms yield

$$\lambda = \frac{2}{\eta_s}\left(\frac{U}{V_j}\right)^2 \tag{B4}$$

Since the blade-jet speed ratio is defined as

$$\upsilon = \frac{U}{V_j}$$

υ is then related to λ by the equation

$$\lambda = 2\,\frac{\upsilon^2}{\eta_s} \tag{B5}$$

From this equation it is evident that, whereas λ is a function of parameters usually considered turbine requirements (specific work and blade speed), the static efficiency is also required to compute υ. Figure 15 presents equation (B5) graphically and is used to compare theoretical and experimental results based on static efficiency.

5048

[redacted]

5048

APPENDIX C

RELATION BETWEEN BLADE LOSS AND TURBINE TOTAL LOSS

In the body of the report, one fundamental assumption made in relating the turbine total efficiency to λ and $V_{u,1}/\Delta V_u$ is that the sum of the stator and rotor losses as defined herein is equal to the turbine specific energy loss $\Delta h'_{id} - \Delta h'$. The validity of this assumption can be described by considering figure 16, where the stator flow characteristics are presented on the familiar enthalpy-entropy diagram.

If the expansion across the stator to the exit static pressure p_1 occurs with no loss, the difference between the total and static enthalpy is

$$h'_0 - h_{id,1} = \frac{V^2_{id,1}}{2gJ} \tag{C1}$$

With the total-pressure loss the difference is

$$h'_0 - h_1 = \frac{V^2_1}{2gJ} \tag{C2}$$

The stator blade loss L_S is defined herein as the difference between the actual and ideal specific kinetic energies occurring as a result of the expansion to p_1. This loss is expressed in units of Btu/lb as

$$L_S = \frac{V^2_{id,1}}{2gJ} - \frac{V^2_1}{2gJ} \tag{C3}$$

or using equations (C1) and (C2)

$$L_S = h_1 - h_{id,1} \tag{C4}$$

A static pressure $p_{id,1}$ is shown in figure 16. This pressure is defined as that necessary to expand isentropically to $V^2_1/2gJ$. Since $V^2_1/2gJ$ is also obtained by expanding isentropically from p'_1 to p_1 with both expansions occurring from h'_0, it follows that

$$\frac{p_1}{p'_1} = \frac{p_{id,1}}{p'_0}$$

or

$$\frac{p_1}{p_{id,1}} = \frac{p_1'}{p_0'} \tag{C5}$$

It is now desired to obtain p_1'/p_0' in terms of L_S. Modifying equation (C4)

$$L_S = h_1 \left(1 - \frac{h_{id,1}}{h_1}\right) \tag{C6}$$

Since isentropic relations hold along the vertical line between points a and b in figure 16,

$$L_S = h_1 \left[1 - \left(\frac{p_1}{p_{id,1}}\right)^{\frac{\gamma-1}{\gamma}}\right] \tag{C7}$$

Solving for $p_1/p_{id,1}$ gives

$$\frac{p_1}{p_{id,1}} = \left(1 - \frac{L_S}{h_1}\right)^{\frac{\gamma}{\gamma-1}} \tag{C8}$$

or expanding and neglecting higher order terms results in

$$\frac{p_1}{p_{id,1}} = 1 - \frac{\gamma}{\gamma-1}\frac{L_S}{h_1} \tag{C9}$$

Then substituting equation (C5) into (C9) yields

$$\frac{p_1'}{p_0'} = 1 - \frac{\gamma}{\gamma-1}\frac{L_S}{h_1} \tag{C10}$$

The loss characteristics of the rotor can be derived in a similar manner. Figure 17 presents the rotor characteristics on the enthalpy-entropy diagram. The total enthalpy level is lower because the flow conditions are relative to the rotor blades. A rotor equation similar to (C10) can be written as

$$\frac{p_2''}{p_1''} = 1 - \frac{\gamma}{\gamma-1}\frac{L_R}{h_2} \tag{C11}$$

Figure 18 presents the over-all turbine performance characteristics on the enthalpy-entropy diagram. Using the same procedure as that applied

to the stator and rotor, an equation for the turbine-outlet conditions similar to equation (C7) can be written as

$$\Delta h'_{id} - \Delta h' = h'_2 \left[1 - \left(\frac{p'_2}{p'_{id,2}} \right)^{\frac{\gamma-1}{\gamma}} \right] \tag{C12}$$

where $p'_{id,2}$ is the turbine-exit total pressure that occurs if $\Delta h'$ is obtained isentropically. By expanding $p'_2/p'_{id,2}$,

$$\frac{p'_2}{p'_{id,2}} = \frac{p'_2}{p''_2} \frac{p''_2}{p''_1} \frac{p''_1}{p'_1} \frac{p'_1}{p'_0} \frac{p'_0}{p'_{id,2}} \tag{C13}$$

Since

$$\frac{p'_2}{p''_2} = \left(\frac{T'_2}{T''_2} \right)^{\frac{\gamma}{\gamma-1}}$$

and

$$\frac{p''_1}{p'_1} = \left(\frac{T''_1}{T'_1} \right)^{\frac{\gamma}{\gamma-1}}$$

then

$$\frac{p'_2}{p''_2} \frac{p''_1}{p'_1} = \left(\frac{T'_2}{T'_1} \right)^{\frac{\gamma}{\gamma-1}} = \frac{p'_{id,2}}{p'_0}$$

As a result, equation (C13) can be written as

$$\frac{p'_2}{p'_{id,2}} = \frac{p''_2}{p''_1} \frac{p'_1}{p'_0} \tag{C14}$$

Substituting equations (C10) and (C11) into equation (C14) gives

$$\frac{p'_2}{p'_{id,2}} = \left(1 - \frac{\gamma}{\gamma-1} \frac{L_S}{h_1} \right) \left(1 - \frac{\gamma}{\gamma-1} \frac{L_R}{h_2} \right)$$

Then by expanding and neglecting second-order terms

$$\frac{p'_2}{p'_{id,2}} = 1 - \frac{\gamma}{\gamma-1} \frac{L_S}{h_1} - \frac{\gamma}{\gamma-1} \frac{L_R}{h_2} \tag{C15}$$

5048

5048

CL-4 back

Substituting equation (C15) into equation (C12) yields

$$\Delta h'_{id} - \Delta h' = h'_2 \left[1 - \left(1 - \frac{\gamma}{\gamma-1} \frac{L_S}{h_1} - \frac{\gamma}{\gamma-1} \frac{L_R}{h_2} \right)^{\frac{\gamma-1}{\gamma}} \right] \tag{C16}$$

Finally, by expanding equation (C16) and neglecting higher order terms

$$\Delta h'_{id} - \Delta h' = \frac{h'_2}{h_1} L_S + \frac{h'_2}{h_2} L_R. \tag{C17}$$

Since, in most turbine cases, the enthalpy ratios in equation (C17) are close to unity, these terms can be neglected resulting in

$$\Delta h'_{id} - \Delta h' = L_S + L_R \tag{C18}$$

REFERENCES

1. Stodola, A.: Steam and Gas Turbines. Vol. I. McGraw-Hill Book Co., Inc., 1927. (Reprinted, Peter Smith (New York), 1945.)

2. Kochendorfer, Fred D., and Nettles, J. Cary: An Analytical Method of Estimating Turbine Performance. NACA Rep. 930, 1949. (Supersedes NACA RM E8I16.)

3. Stewart, Warner L., and Evans, David G.: Analytical Study of Losses at Off-Design Conditions for a Fixed-Geometry Turbine. NACA RM E53K06, 1954.

4. Stenning, Alan H.: Design of Turbines for High-Energy-Fuel Low-Power-Output Applications. Rep. No. 79, Dynamic Analysis and Control Lab., M.I.T., Sept. 30, 1953.

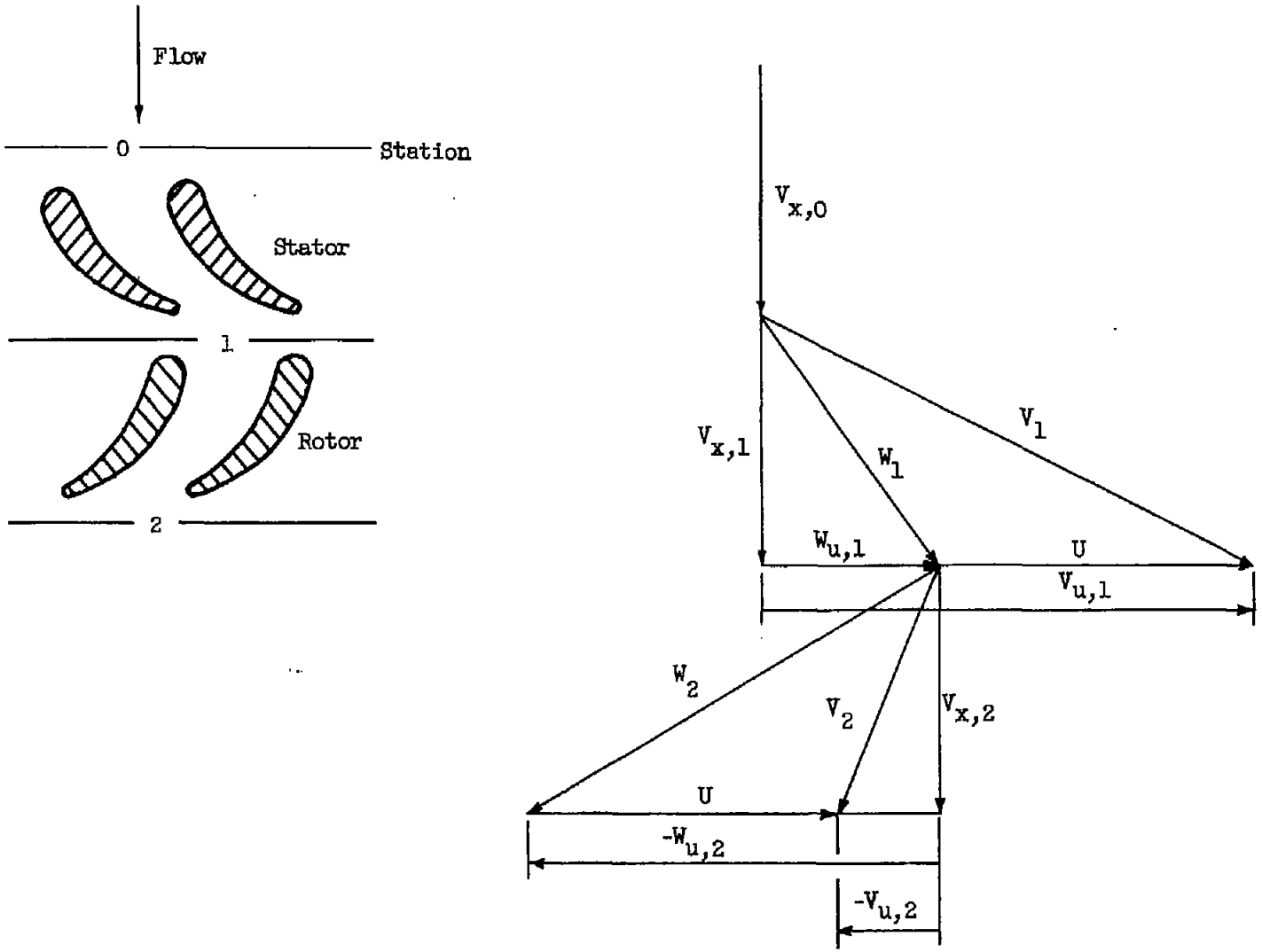

Figure 1. - Velocity diagrams and nomenclature.

5048

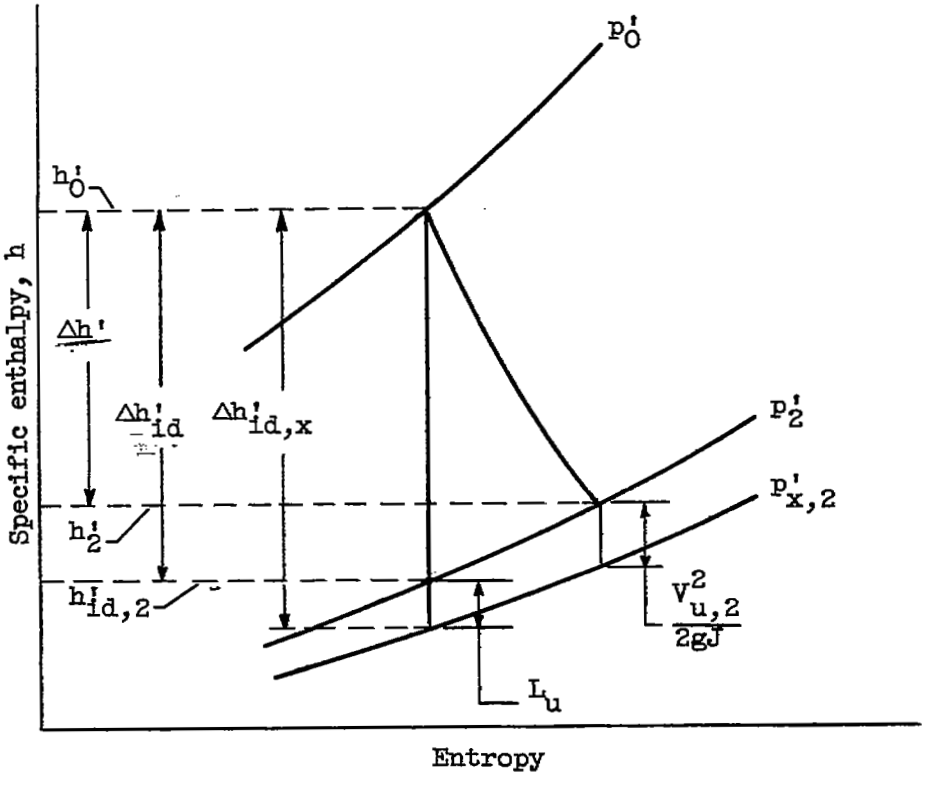

Figure 2. - Single-stage-turbine characteristics on enthalpy-entropy diagram.

5048

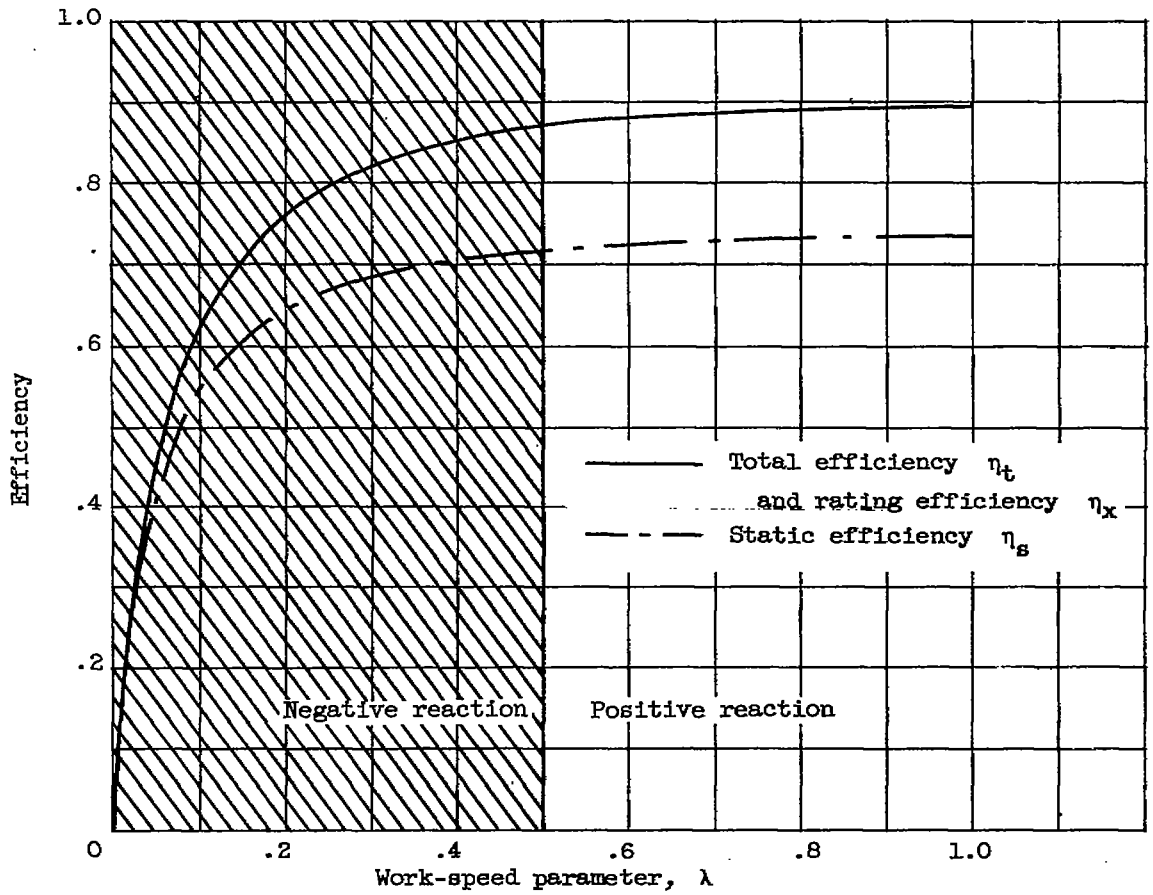

Figure 3. - Efficiency characteristics for zero exit whirl.

$\frac{(V_x^2)_{av}}{gJ\Delta h'} = 0.49$; B = 0.030.

5048

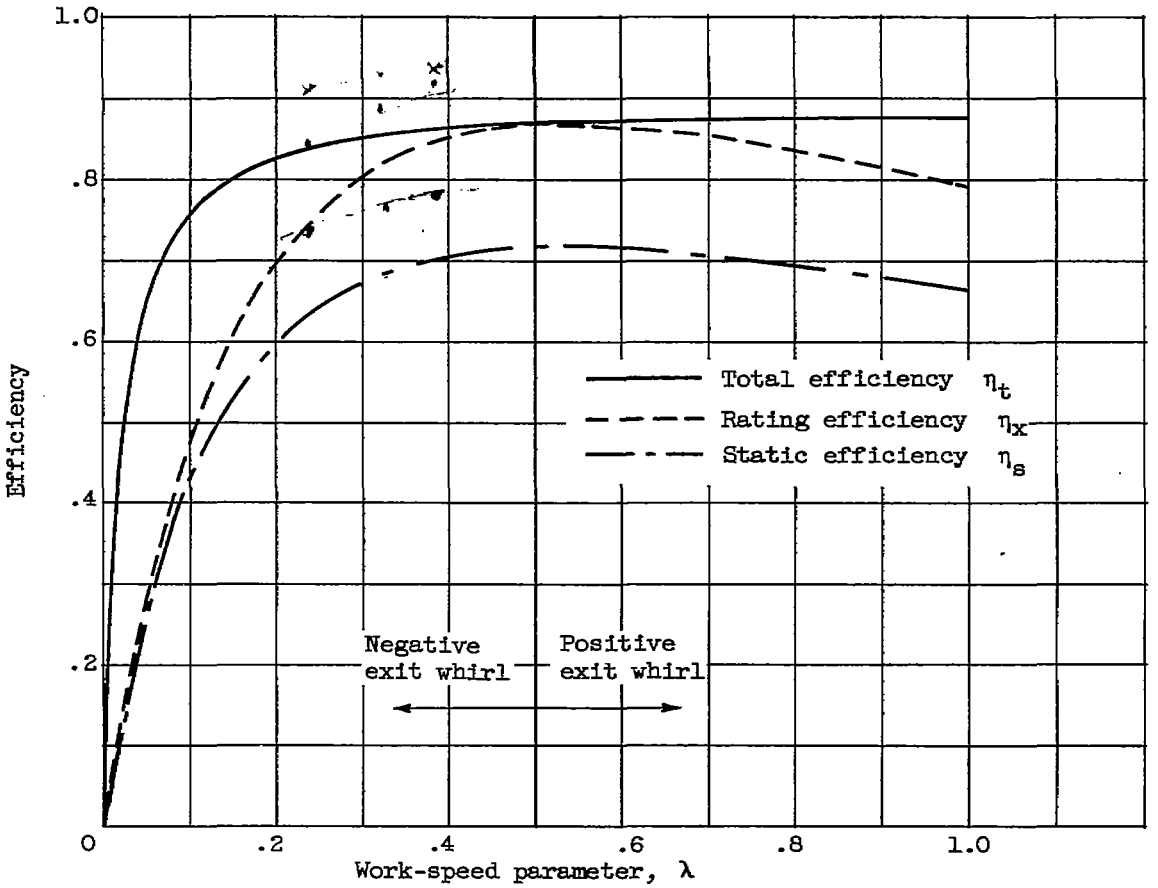

Figure 4. - Efficiency characteristics for impulse conditions. $\frac{(V_x^2)_{av}}{gJ\Delta h'} = 0.49$; B = 0.030.

5048

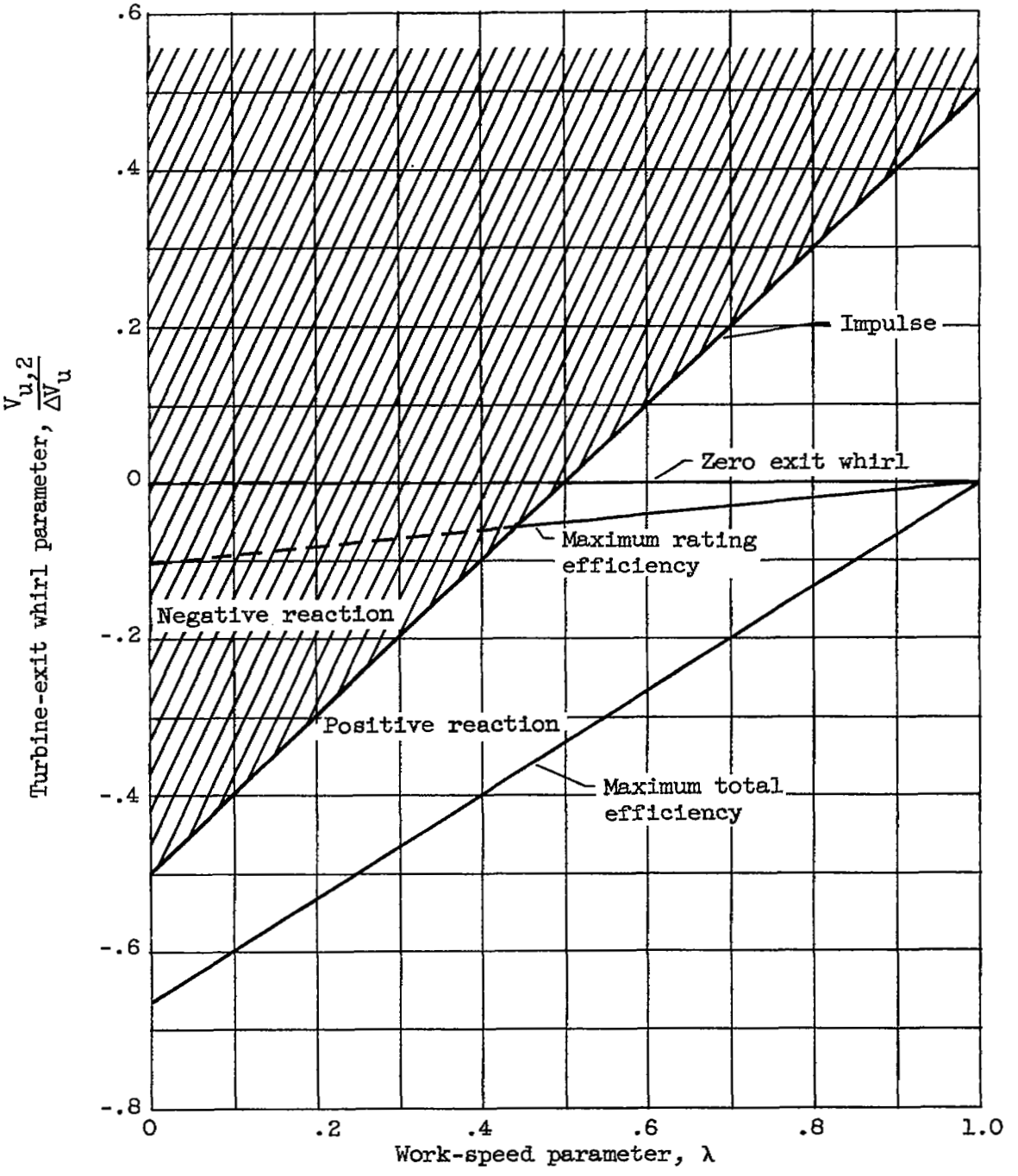

Figure 5. - Turbine-exit whirl characteristics for specified velocity diagram conditions.

[redacted]

CL-5 5048

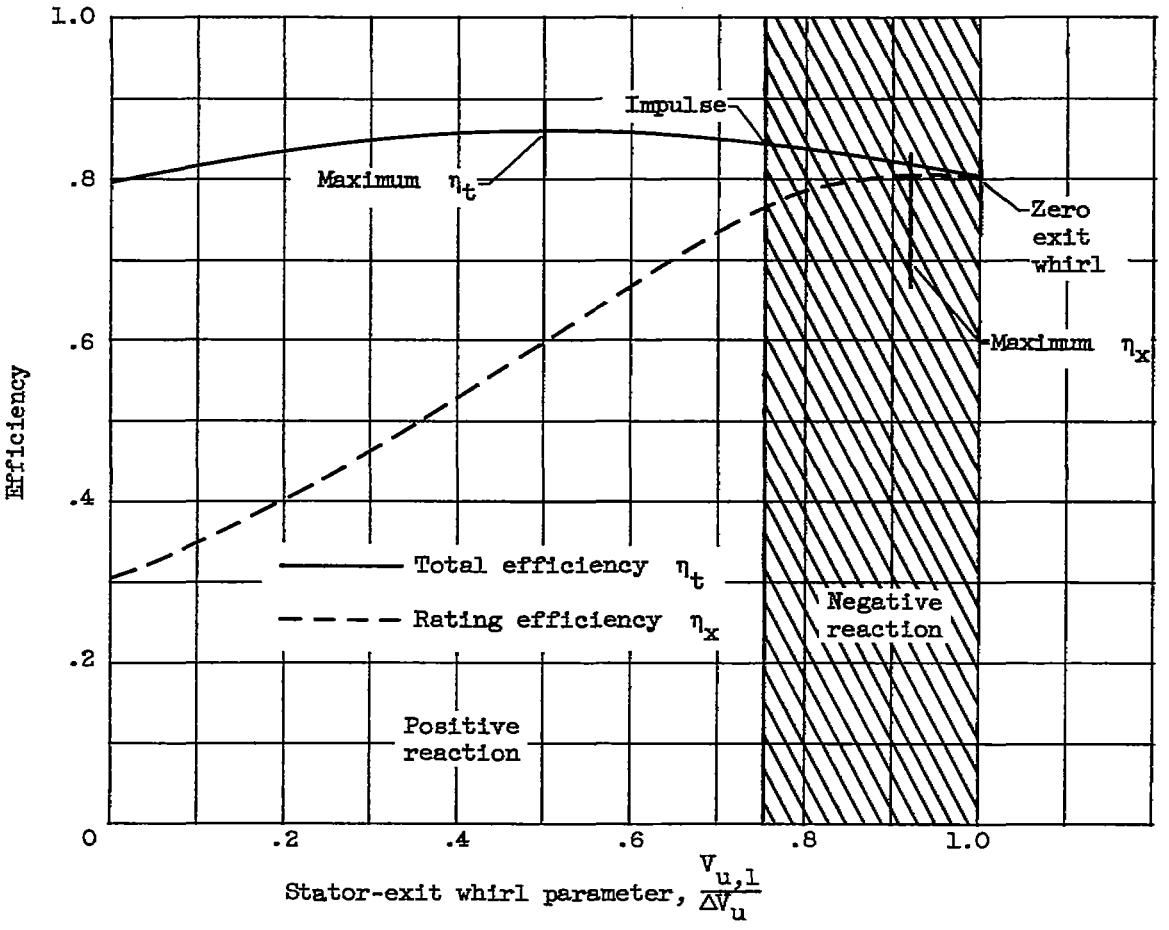

Figure 6. - Typical variation in efficiency with stator-exit whirl parameter. Work-speed parameter λ, 0.25.

5048

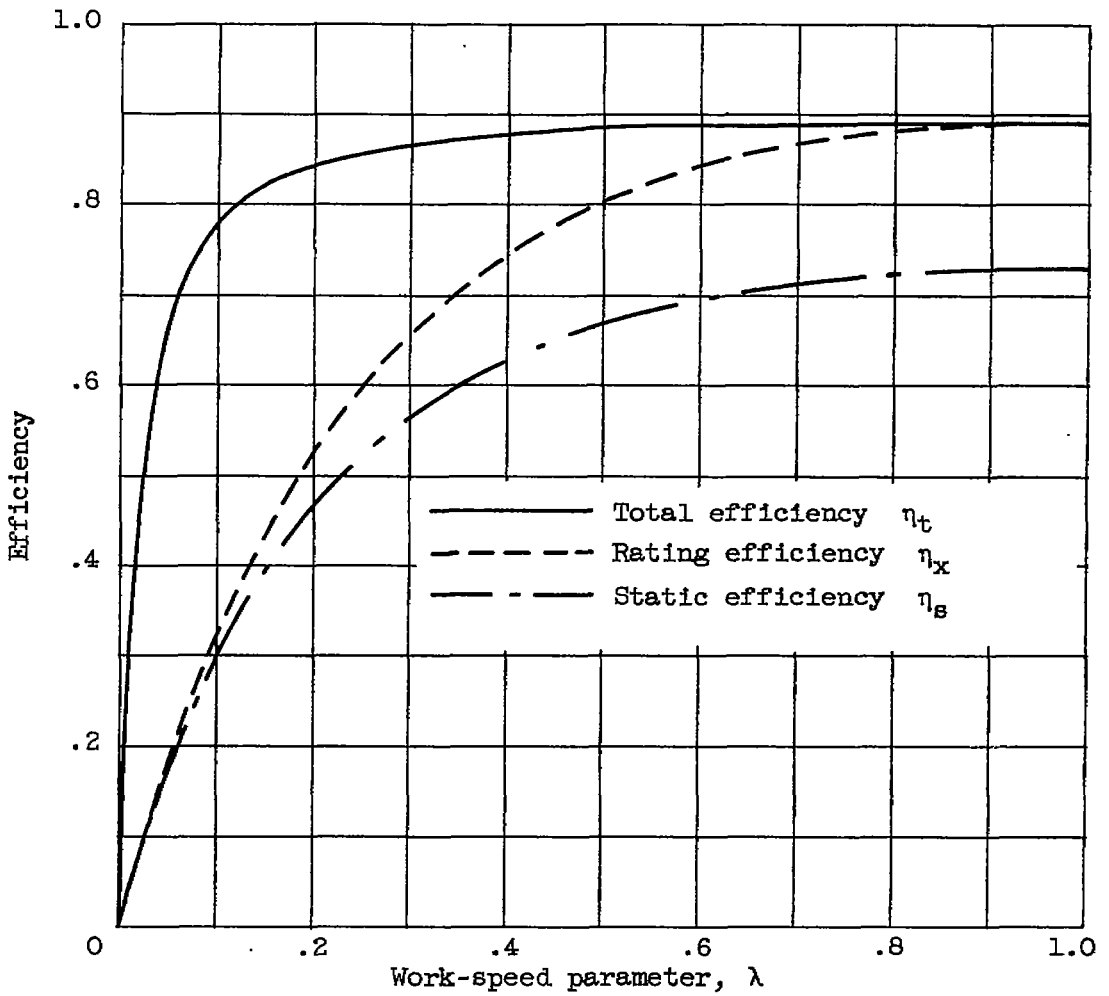

Figure 7. - Maximum total efficiency characteristics. $\frac{(V_x^2)_{av}}{gJ\Delta h'} = 0.49$; B = 0.030.

CL-5 back 5048

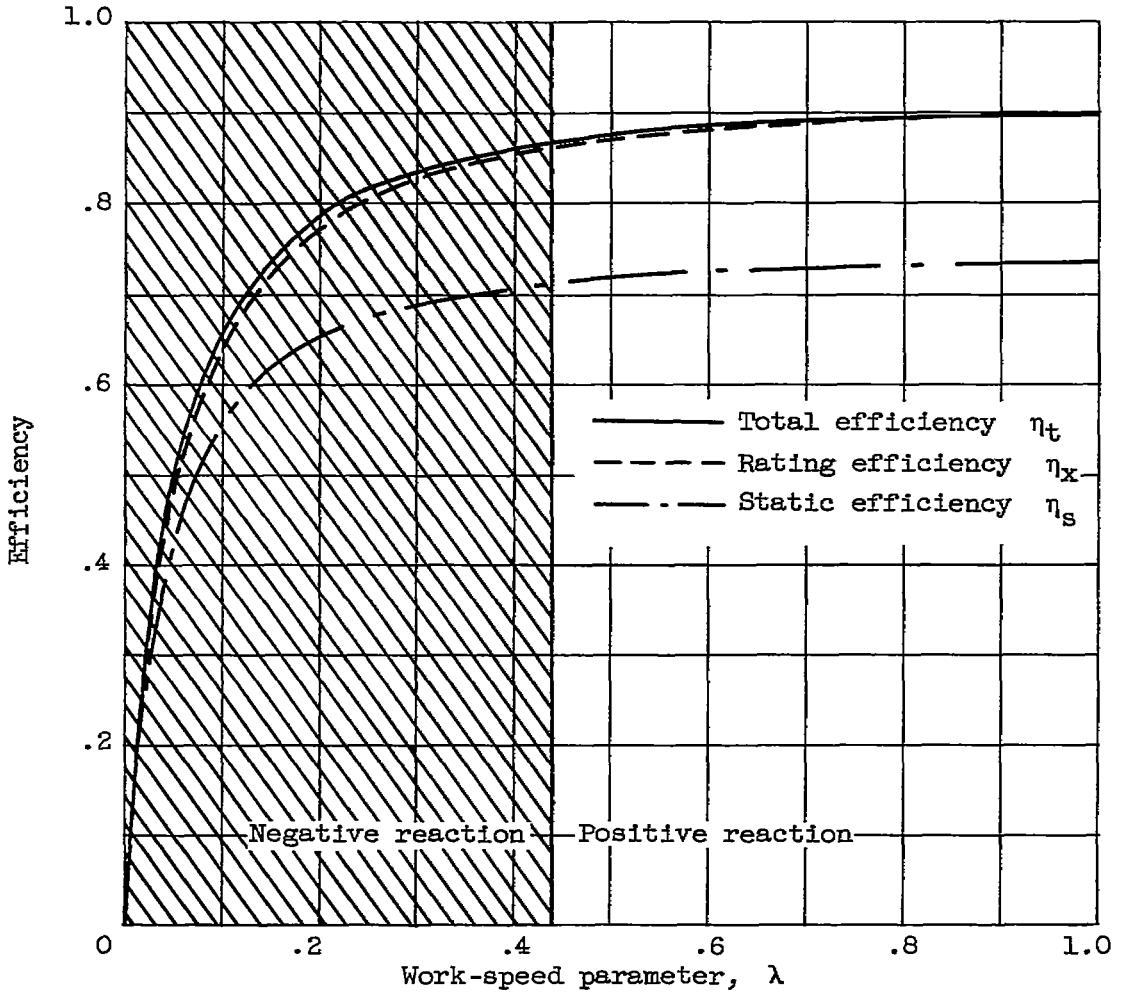

Figure 8. - Maximum rating efficiency characteristics. $\frac{(V_x^2)_{av}}{gJ\Delta h'} = 0.49$; B = 0.030.

[redacted]

5048

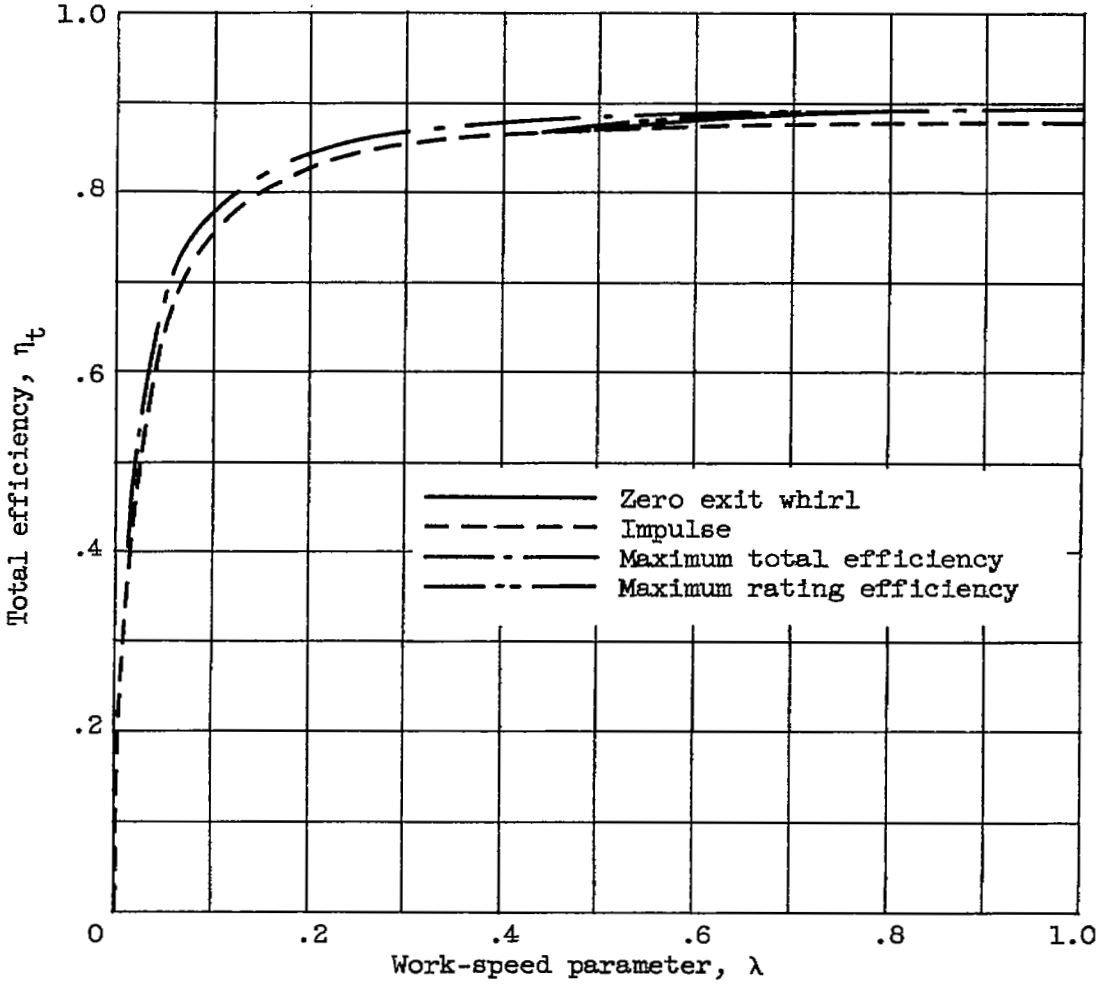

Figure 9. - Total efficiency comparison. $\frac{(V_x^2)_{av}}{gJ\Delta h'} = 0.49$; B = 0.030.

5048

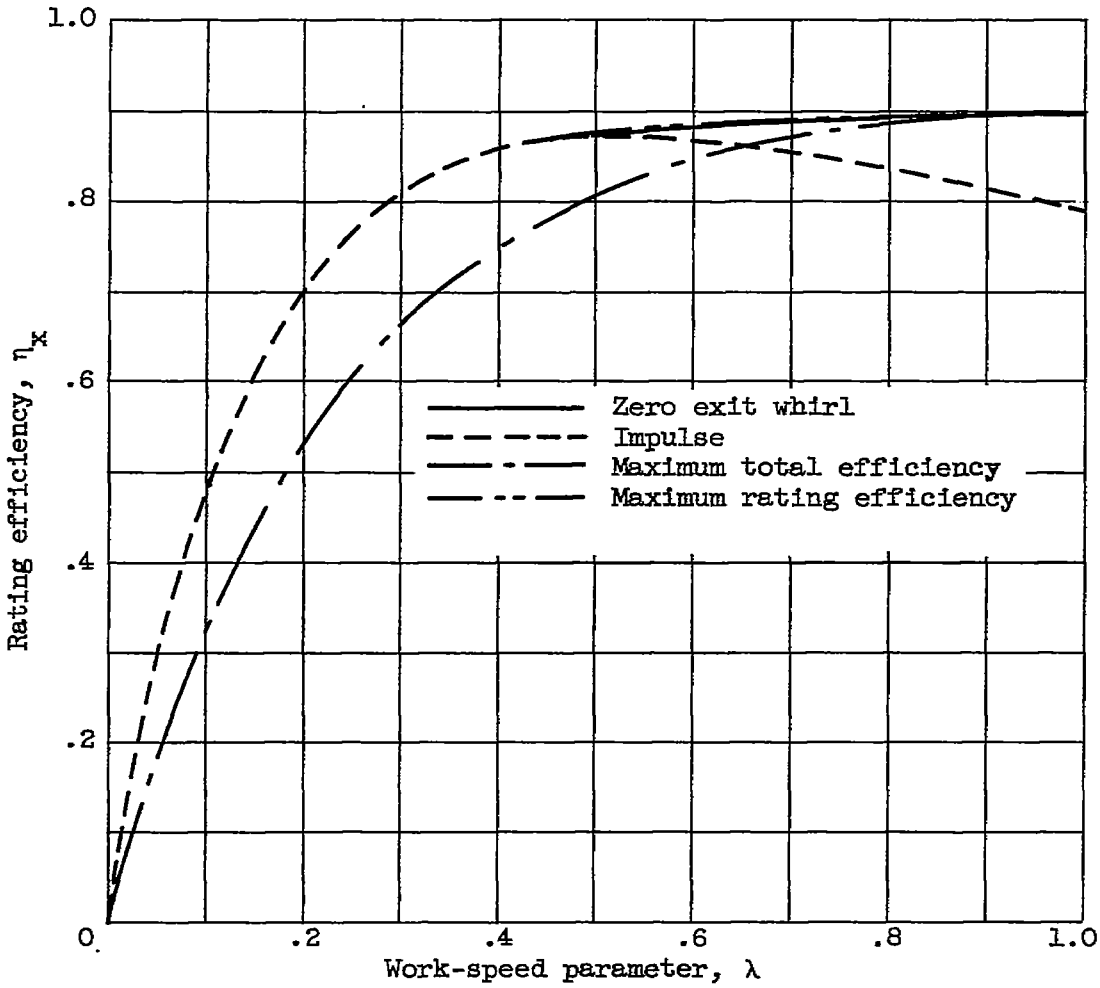

Figure 10. - Rating efficiency comparison. $\frac{(V_x^2)_{av}}{gJ\Delta h'} = 0.49$; B = 0.030.

5048

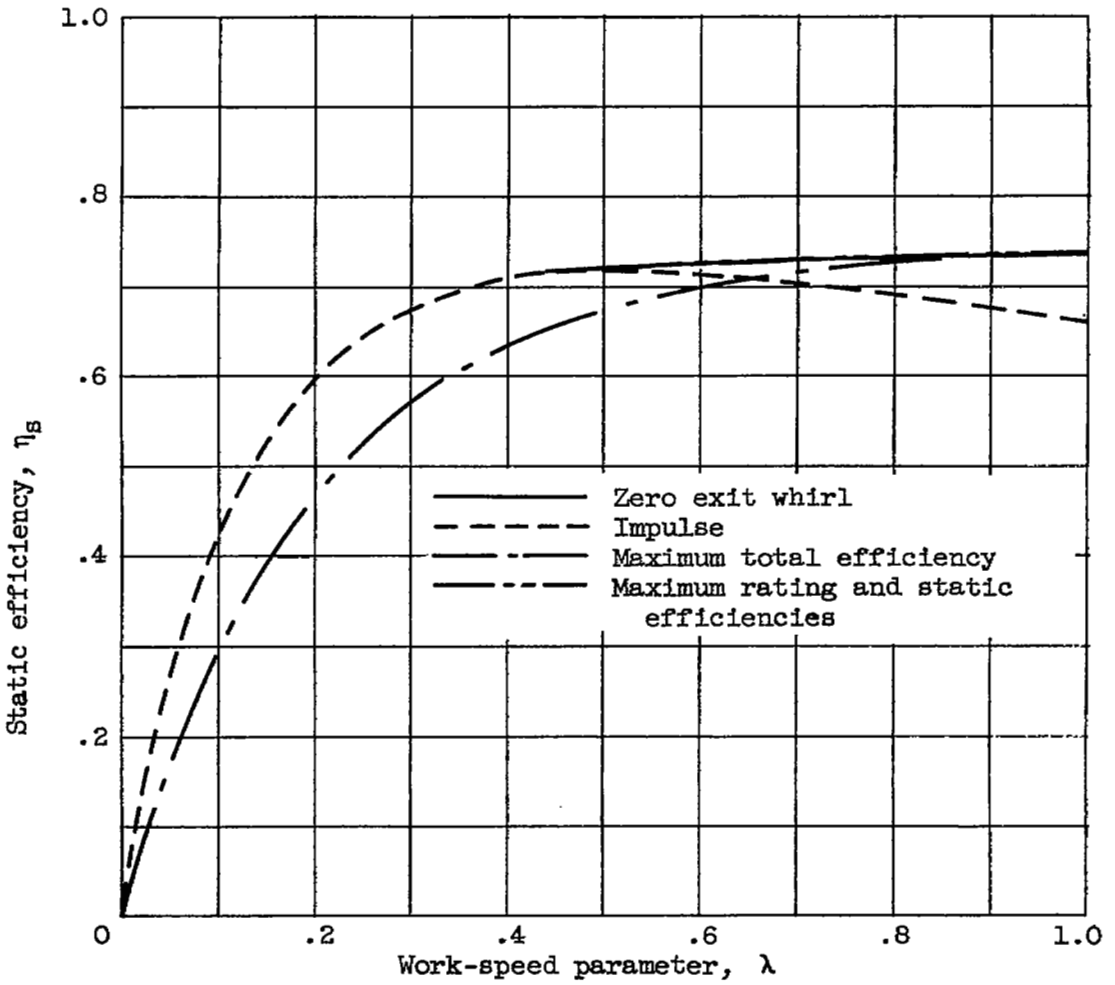

Figure 11. - Static efficiency comparison. $\frac{(V_{x\,av}^2)}{gJ\Delta h'} = 0.49$; B = 0.030.

[redacted]

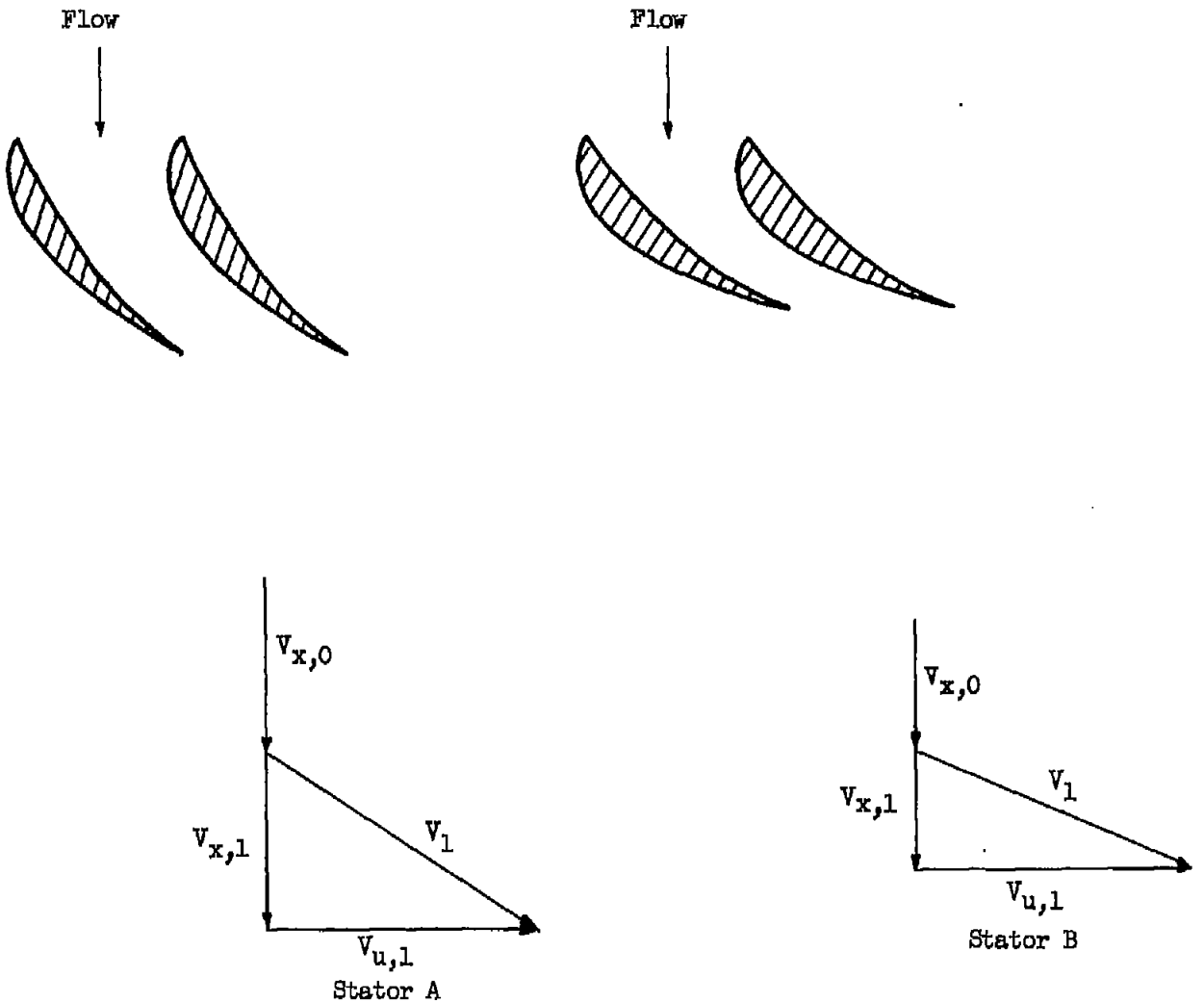

Figure 12. - Example effect of reduction in weight-flow level on blade surface area and velocity diagram characteristics.

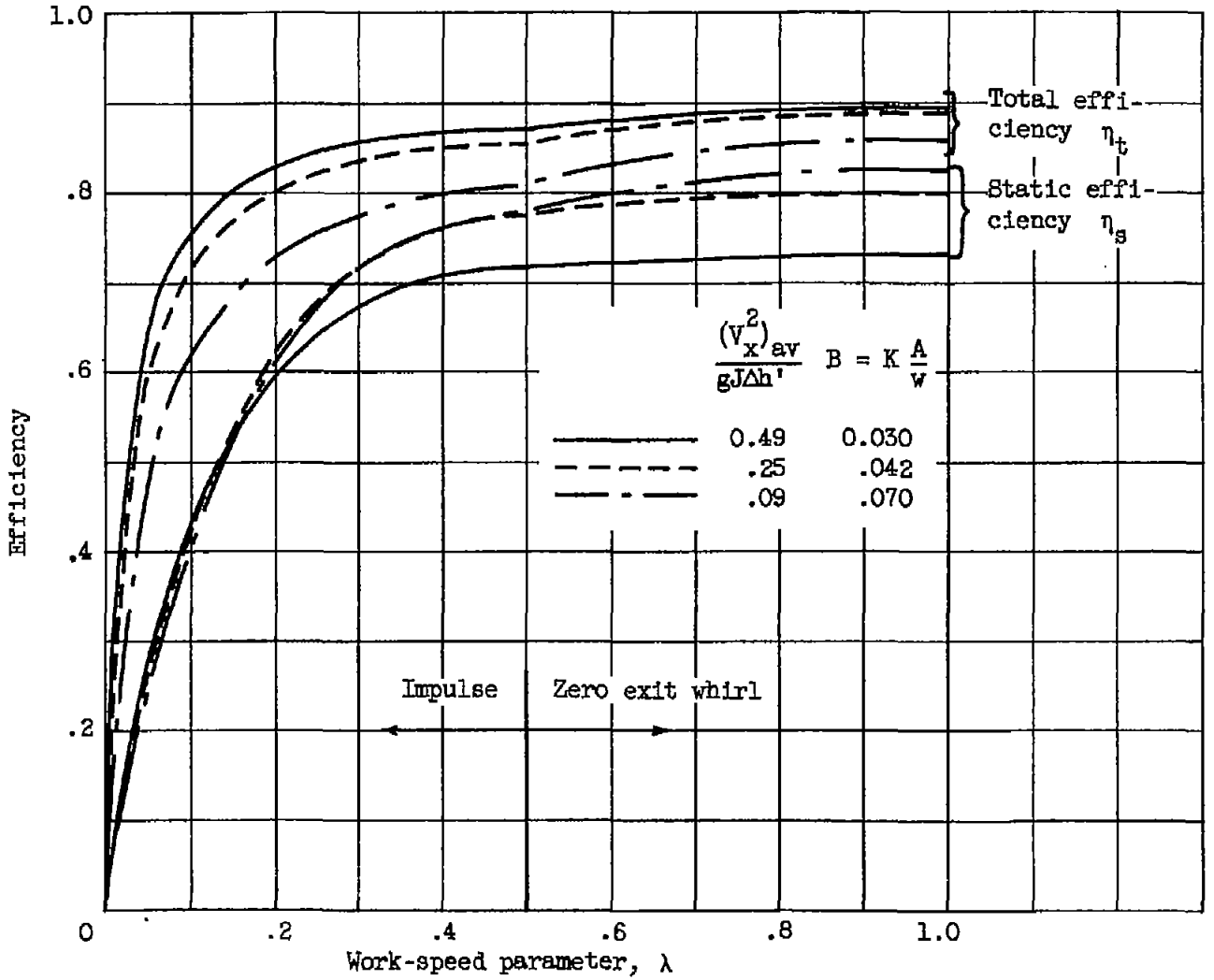

Figure 13. - Effect of varying axial velocity parameter on total and static efficiency characteristics.

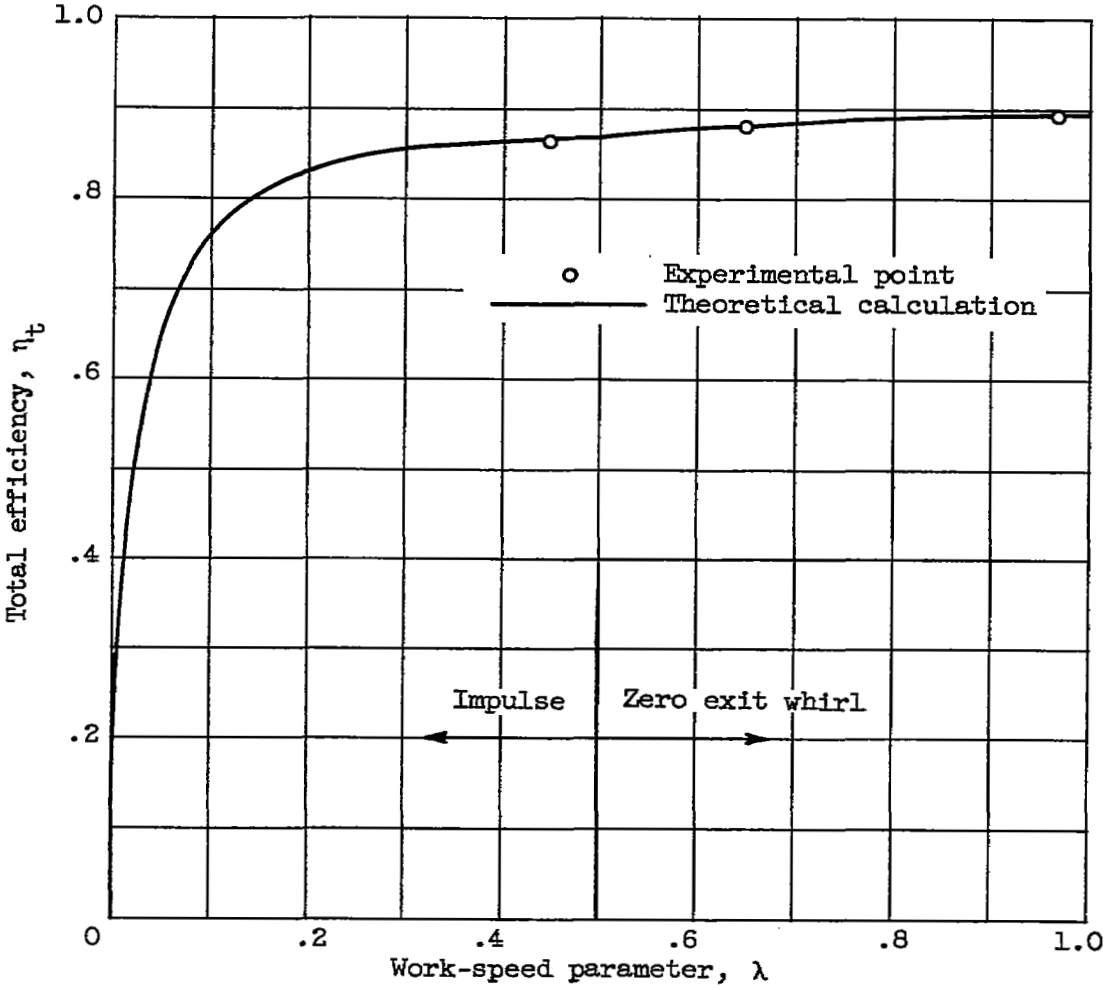

Figure 14. - Comparison of theoretical results with single-stage cold-air turbine tests. $\frac{(V_x^2)_{av}}{gJ\Delta h'} = 0.49$; B = 0.030.

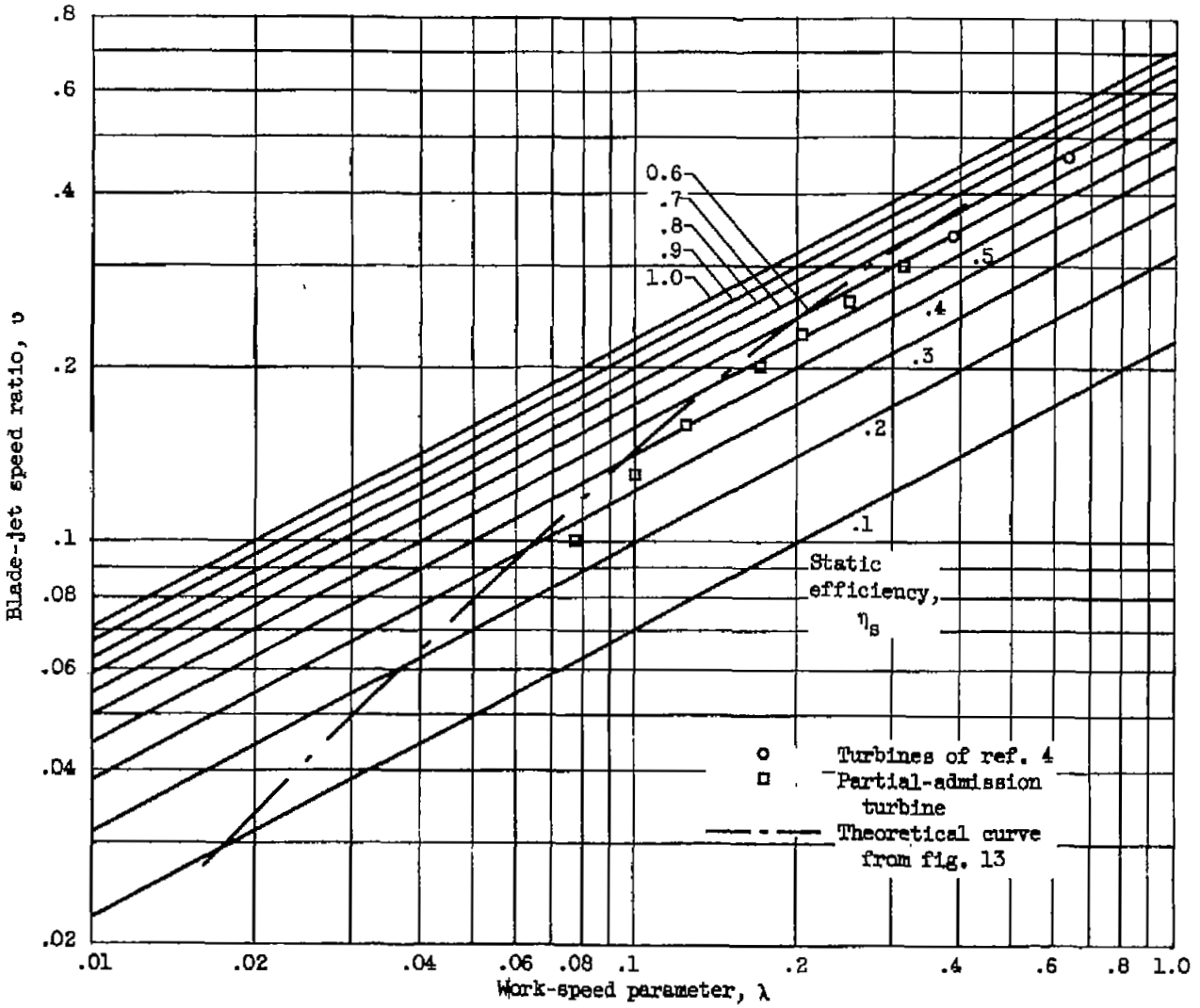

Figure 15. - Variation in blade-jet speed ratio with work-speed parameter including calculated static efficiency characteristics and experimental comparison.

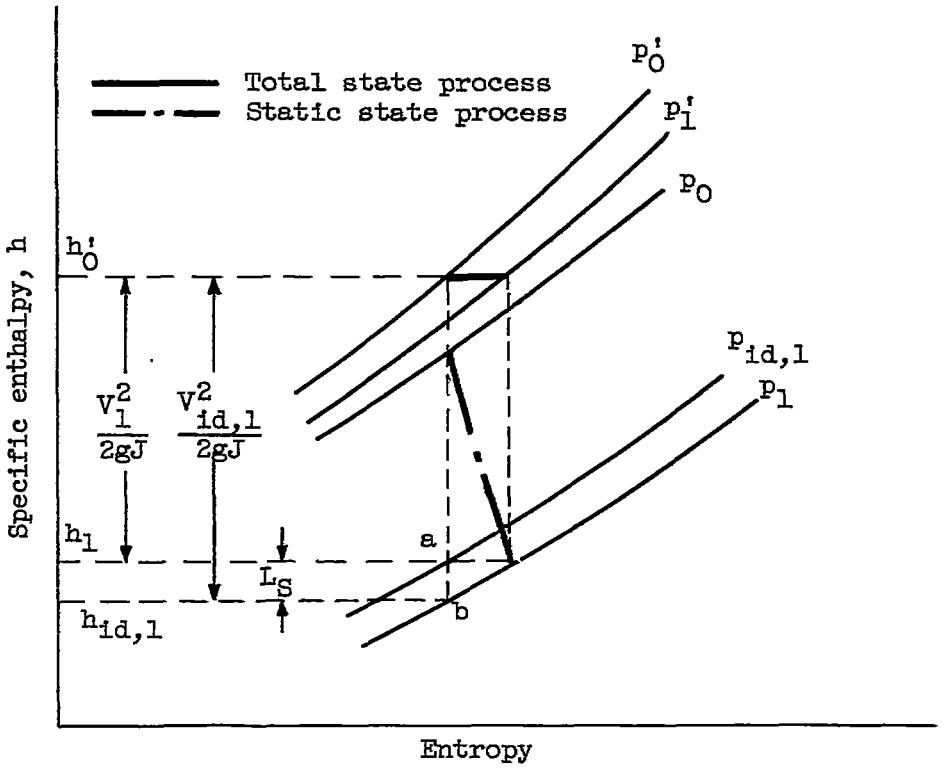

Figure 16. - Stator loss characteristics on enthalpy-entropy diagram.

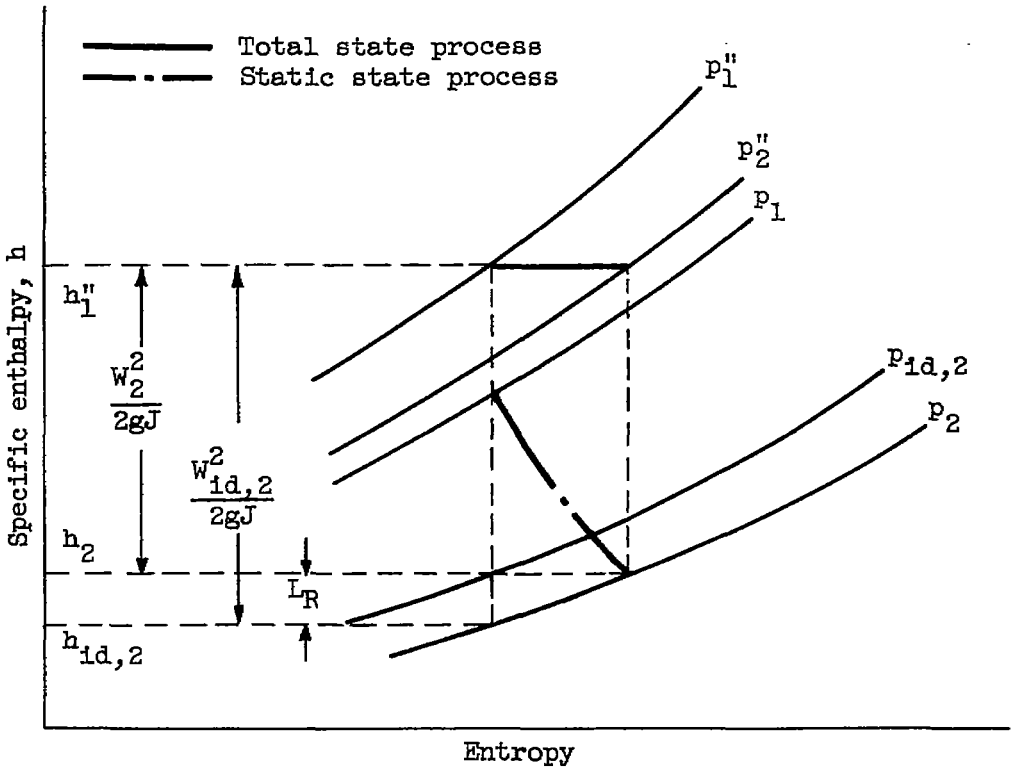

Figure 17. - Rotor loss characteristics on enthalpy-entropy diagram.

5048

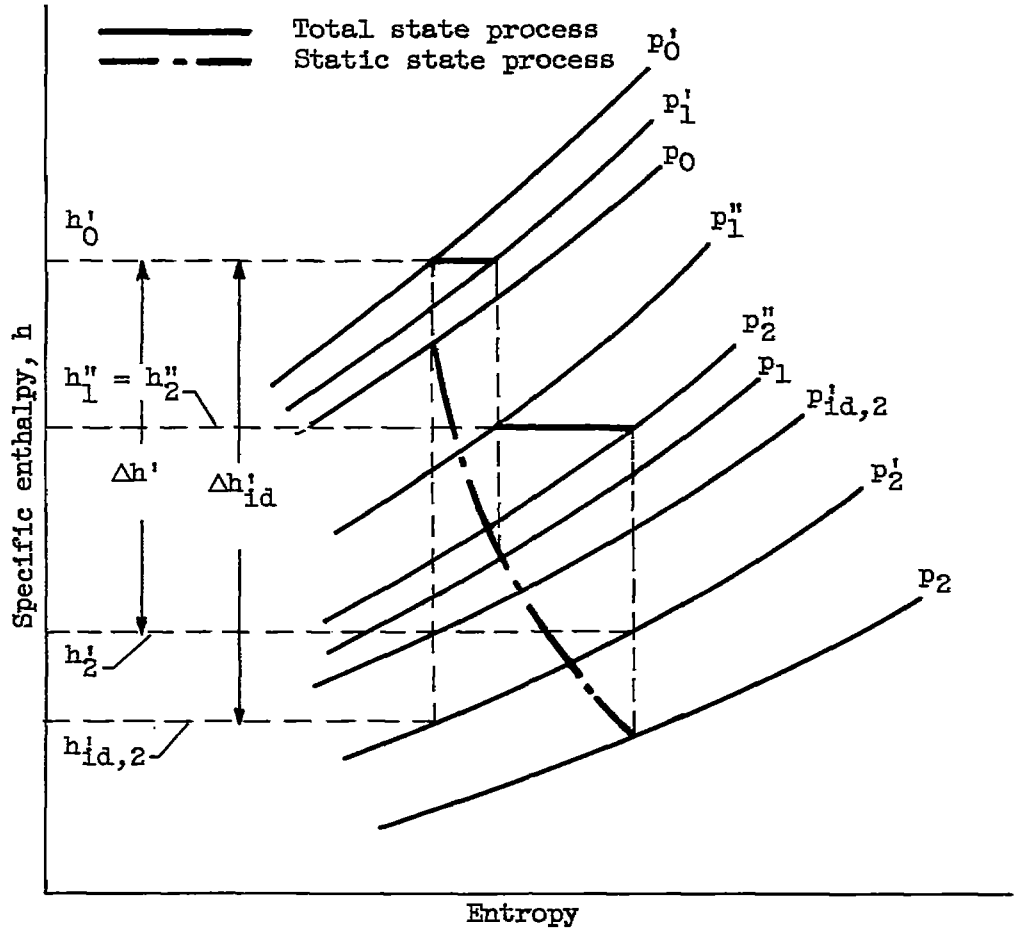

Figure 18. - Turbine loss characteristics on enthalpy-entropy diagram.

NASA Technical Library
3 1176 01436 1076